

THE ROOM TEMPERATURE IONIC LIQUID-BASED SYNTHESIS AND
CHARACTERIZATION OF POLYOXOMOLYBDATE COMPOUNDS

By

STEPHEN L LINGUITO

A thesis submitted to the

Graduate School–New Brunswick

Rutgers, The State University of New Jersey

in partial fulfillment of the requirements

for the degree of

Master of Science

Graduate Program in Chemistry

written under the direction of

Professor Jing Li

and approved by

New Brunswick, New Jersey

January 2011

ABSTRACT OF THE THESIS

The Room Temperature Ionic Liquid-Based Synthesis and Characterization of Polyoxomolybdate Compounds

by STEPHEN L LINGUITO

Thesis Director:

Professor Jing Li

Polyoxometalates which feature anionic metal clusters are promising materials for a wide variety of applications. One specific area of research that has received relatively limited attention has been the synthesis of polyoxomolybdate compounds (one type of polyoxometalate) involving the use of room temperature ionic liquids. In this context, the synthesis of three polyoxomolybdate materials from a room temperature ionic liquid will be discussed.

The usage of the ionic liquid 1-butyl-3-methyl-imidazolium tetrafluoroborate, (bmim)[BF₄], allowed for the synthesis of (bmim)₃NH₄[Mo₈O₂₆], (bmim)₄[PMo^VMo₁₁O₄₀], and (bmim)₃[PMo₁₂O₄₀], via the *in situ* incorporation of the organic imidazolium cation of the ionic liquid. This synthetic approach offers the additional benefit of being “green” in nature. The ionothermal reactions discussed feature the use of glass vials and acid digestion bombs as reaction vessels, relatively mild conditions, and simple molybdate salts.

Details related to the characterization of these compounds will be presented. A discussion of the catalytic role that (bmim)₃[PMo₁₂O₄₀] plays in the oxidation of styrene to benzaldehyde will also be conducted.

ACKNOWLEDGEMENTS

To start, I wish to thank my thesis director Dr. Jing Li for accepting me into her research group, and for all the help and guidance she has provided. Her hard work and passion for chemistry should serve as an inspiration to all of us.

I wish to thank my thesis committee members Dr. KiBum Lee and Dr. Ralf Warmuth for their contributions to this work.

Thanks are extended to Dr. Xiaoying Huang and especially to Dr. Thomas J. Emge for their contributions, their expertise, and their efforts in crystallographically solving the structures presented in this work.

I thank Dr. Ankush Biradar, a postdoctoral fellow in Dr. Asefa's research group, for taking an interest in my work, for running catalysis experiments with the samples I provided to him, for analyzing the results, and in general for sharing his catalysis expertise.

Special thanks are in order for Dr. Moothetty Padmanabhan, a visiting scholar with whom I worked closely. His assistance was offered both enthusiastically and generously. I learned many things from him, and this work would simply not be possible without him. I would also like to thank Dr. Yonggang Zhao for taking over from where Dr. Padmanabhan left off.

I would like to thank Samantha Levine, a visiting high school student who worked in Dr. Li's lab in 2003. She laid the foundation for the research presented in this work. Thanks are also extended to the numerous group members I have had the privilege of interacting with during my time in Dr. Li's lab. Whenever I had a question or needed help, they were always there.

Last but not least, I would like to extend my deepest thanks to my parents for their unconditional love and support.

The introduction presented in this thesis was adapted from the introduction of a journal article manuscript whose publication in *Crystal Growth & Design* is forthcoming.

DEDICATION

To

Irene, My Mother

And Leonard, My Father

TABLE OF CONTENTS

Title Page.....	i
Abstract.....	ii
Acknowledgements.....	iii
Dedication.....	v
Table of Contents.....	vi
List of Tables.....	vii
List of Illustrations.....	viii
List of Abbreviations.....	x
Introduction.....	1
Chapter 1. Historical polyoxomolybdates.....	11
(bmim) ₃ NH ₄ [Mo ₈ O ₂₆].....	12
(bmim) ₄ [PMo ^V Mo ₁₁ O ₄₀].....	17
Summary.....	24
Chapter 2. A new polyoxomolybdate.....	26
(bmim) ₃ [PMo ₁₂ O ₄₀].....	28
Summary.....	43
Experimental.....	45

LIST OF TABLES

Chapter 1

Table 2-1 Crystal Data for $(\text{bmim})_3\text{NH}_4[\text{Mo}_8\text{O}_{26}]$15

Table 2-2 Crystal Data for $(\text{bmim})_4[\text{PMo}^{\text{V}}\text{Mo}_{11}\text{O}_{40}]$20

Chapter 2

Table 3-1 Crystal Data for $(\text{bmim})_3[\text{PMo}_{12}\text{O}_{40}]$31

Table 3-2 Crystal data comparison of **2** and **3**.....37

Table 3-3 Results of styrene oxidation reactions.....40

LIST OF ILLUSTRATIONS

Introduction

- Fig. 1-1. The number of published articles containing the phrase “ionic liquid” as entered, according to a Scifinder survey conducted on July 24, 2010.....2
- Fig. 1-2. A view of **1** along the crystallographic *b*-axis showing parallel-stacked [Cu(bpp)]⁺ layers and BF₄⁻ anions located between these layers. Boron atoms are in red and fluorine atoms, in light-blue.³⁴4
- Fig. 1-3. The structure of the {Mo₃₆₈} ‘lemon’ cluster. The side view is shown (LHS) and the top view is also shown (RHS).⁶¹6

Chapter 1

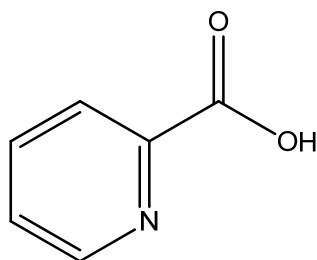
- Fig. 2-1. View of the unit cell of **1** projected along the
- (a) x axis.....13
 - (b) y axis.....13
 - (c) z axis.....13
- Fig. 2-2. (a) PXRD pattern for **1**.....16
- (b) TGA plot for **1**.....16
- Fig. 2-3. View of the unit cell of **2** projected approximately along the
- (a) x axis.....18
 - (b) y axis.....18
 - (c) z axis.....18
- Fig. 2-4. (a) TGA plot for **2**.....22
- (b) PXRD pattern for **2**, corresponding to Scheme 3-2 reaction.....22
 - (c) PXRD pattern for **2**, corresponding to Scheme 3-3 reaction.....22

Chapter 2

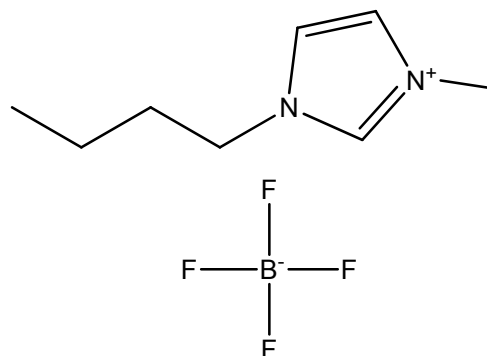
Fig. 3-1. ORTEP drawing of 1 showing the labeling of atoms with thermal ellipsoids at 50% probability. Hydrogen atoms are omitted for clarity. ¹	27
Fig. 3-2. View of the unit cell of 3 projected approximately along the	
(a) x axis	29
(b) y axis	29
(c) z axis	29
Fig. 3-3. Percent improvement in yield of compound 3 as a function of the copper to molybdenum ratio	33
Fig. 3-4. (a) PXRD pattern for 3	36
(b) UV spectrum for 3	36
(c) TGA plot for 3	36
Fig. 3-5. Schematic representation of the reaction performed using compound 3 as an oxidation catalyst	38
Fig. 3-6. PXRD pattern of compound 3 before oxidation reactions, after one oxidation reaction, and after five oxidation reactions	41
Fig. 3-7. (a) TGA plot for unused compound 3 material	41
(b) TGA plot for compound 3 material used in five catalysis reactions	41

LIST OF ABBREVIATIONS AND STRUCTURES

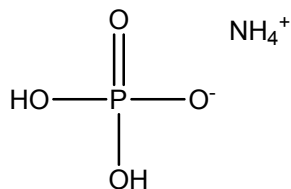
I. Selected chemical abbreviations and structures



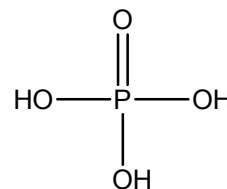
2-pca 2-pyridinecarboxylic acid



(bmim)[BF₄] 1-butyl-3-methyl-imidazolium-tetrafluoroborate



NH₄H₂PO₄ Ammonium phosphate monobasic



H₃PO₄ Phosphoric acid

II. Abbreviations used in this document

1D	One-Dimensional
2D	Two-Dimensional
ACS	American Chemical Society
bmim	1-butyl-3-methyl-imidazolium
bpp	1,3-bis-(4-pyridyl)-propane
emim	1-ethyl-3-methyl-imidazolium
LHS	Left Hand Side
MOF	Metal-Organic Framework

ORTEP	Oak Ridge Thermal Ellipsoid Plot
PXRD	Powder X-Ray Diffraction
RHS	Right Hand Side
RT	Room Temperature
RTIL	Room Temperature Ionic Liquid
TGA	Thermogravimetric Analysis
UV	Ultraviolet
VOC	Volatile Organic Compound

INTRODUCTION

In the past 20 years, interest in ionic liquids has increased explosively. The reasons for this increase in popularity will be detailed in this section. Figure 1-1 illustrates how quickly the literature related to ionic liquids has expanded between 1990 and 2010.

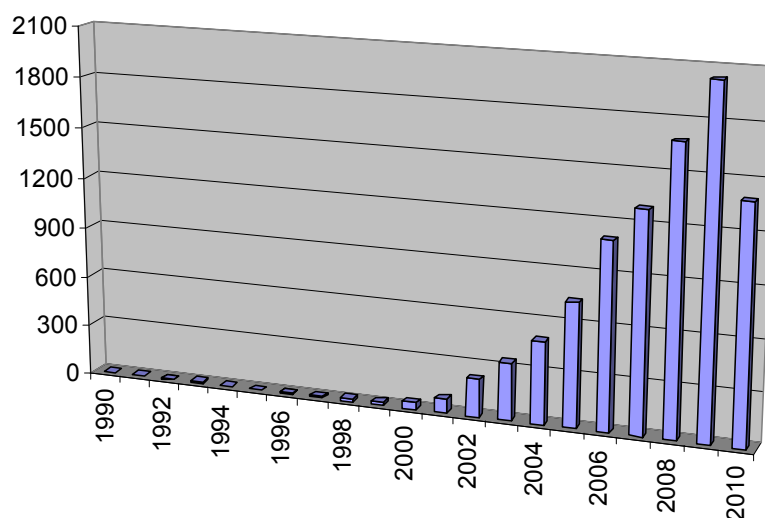


Figure 1-1. The number of published articles containing the phrase “ionic liquid” as entered, according to a Scifinder survey conducted on July 24, 2010.

Characteristic Properties of Ionic Liquids

Room temperature ionic liquids (commonly abbreviated RTILs) are liquids made only from ions that exist as liquids below 373 K.^{1,2} RTILs commonly consist of either imidazolium or pyridinium cations, and various anionic moieties. These types of ionic liquids are aprotic, but there are also protic ionic liquids, such as ethylammonium nitrate. RTILs have attracted considerable attention as highly useful and versatile solvents because of their many unique properties.³⁻¹⁰ They are non-volatile, non-flammable, and are often non-coordinating. They possess high ionic conductivities, wide liquid ranges (sometimes exceeding 400 degrees Celsius), and good solubilizing characteristics. They are tolerant of strong acids, thermally and chemically stable, and can be recovered, purified and reused.

They have wide electrochemical windows, which allow them to be inert in common redox ranges, and they are capable of facilitating the self-assembly of amphiphiles. The usage of RTILs in synthesis is thus considered environmentally-friendly and also safer than hydrothermal and solvothermal reactions carried out in traditional organic solvents. Considering these properties, as well as their volatile organic compound (VOC) replacement ability, and their role in clean separation processes, these solvents can be characterized as highly 'green' for almost all applications.^{6,11-15} The above-mentioned characteristics, along with the coexistence of ionic and organic components, make RTILs unique reaction media for performing a wide variety of novel reactions (organic, organometallic, and inorganic) and catalytic conversions, which are not otherwise possible.^{1,16-22} In addition to being used in the synthesis of novel materials, RTILs have also been employed in mesoscopic dye-sensitized solar cells^{21,23-30} and in biological systems.³¹

Use of Ionic Liquids in Synthesis

RTILs can potentially be used as solvents in the synthesis of materials which possess unique properties, such as zeolites, metal-organic frameworks (MOFs) and inorganic-organic hybrid compounds. In the formation of these materials, the role of structure directing agent or templating agent is quite important, and in ionothermal synthesis RTILs have been observed to behave as solvents and template providers simultaneously. High product specificity can be achieved because this synthetic strategy often removes the competition between template-framework and solvent-framework interactions that is present in conventional hydrothermal or solvothermal syntheses. Molecular modeling studies have shown that the structures of ionic liquids are often characterized by long-range correlations and distributions that reflect the asymmetric structures of their cations. Such long-range asymmetric effects can

potentially increase the likelihood of passing chemical information from the template cation to the framework, which is often desirable, if full control over the templating process must be achieved.^{32,33}

Jin et al reported the first RTIL-based synthesis of a coordination polymer of composition $\text{Cu}(\text{bpp})\text{BF}_4$, where bpp stands for 1,3-bis-(4-pyridyl)-propane. The RTIL 1-butyl-3-methyl-imidazolium tetrafluoroborate ($(\text{bmim})[\text{BF}_4]$) was used as the solvent. The synthesis involved the *in situ* reduction of Cu(II) to form the Cu(I)-based 2D polymer in which the BF_4 of the ionic liquid was incorporated as a charge-compensating anion (Figure 1-2).³⁴ Following this pioneering work, several studies demonstrated the structure-directing role that the cationic and anionic moieties of RTILs can play in the formation of interesting coordination polymers.^{11,35-45} The possibility of intimately-controlled crystallization processes and the formation of new supramolecular architectures has also been demonstrated in these non-volatile liquids.¹¹

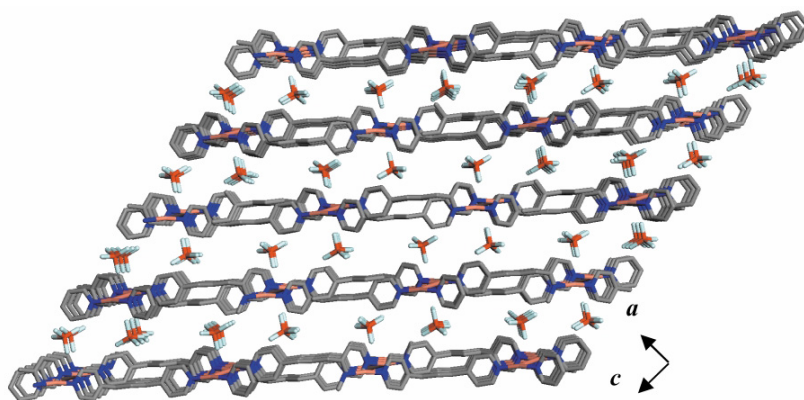


Fig. 1-2. A view of **1** along the crystallographic *b*-axis showing parallel-stacked $[\text{Cu}(\text{bpp})]^+$ layers and BF_4^- anions located between these layers. Boron atoms are in red and fluorine atoms, in light-blue.³⁴

The formation characteristics and structural features of interesting zeo-type materials, aluminophosphates and metal aluminophosphates have also been studied in RTIL-based synthesis, as well as the role of water and other mineralizers in structure formation.^{33,46-49} There have also been attempts to synthesize nano-sized materials in RTILs, and to study the role that these liquids play on the nature and characteristics of such materials.^{2,50-60}

Polyoxometalates

The Mo-, W- and V-based polyoxometalate (POM) compounds are a family of structures that have been intensely studied. Specifically, several types of polyoxomolybdate clusters have been synthesized and structurally characterized. These include $[\text{Mo}_6\text{O}_{19}]$, $[\text{Mo}_8\text{O}_{26}]$, $[\text{Mo}_{10}\text{O}_{36}]$, $[\text{PMo}_{12}\text{O}_{40}]$, the ball-shaped $([\text{Mo}_{132}\text{O}_{372}(\text{MeCO}_2)_{30}(\text{H}_2\text{O})_{72}]^{42-})$, the ring-shaped $([\text{Mo}_{154}\text{O}_{462}\text{H}_{14}(\text{H}_2\text{O})_{70}]^{14-})$, the ring-shaped $([\text{Mo}_{176}\text{O}_{528}\text{H}_{16}(\text{H}_2\text{O})_{80}]^{16-})$, and even a lemon-shaped cluster (Figure 1-3) made from 368 Mo atoms which carries an overall negative charge of 48.⁶¹⁻⁷² All of these clusters are anionic in nature. Water is often used as the solvent in the synthesis of such compounds. Most commonly, the Mo ions are in their usual +6 oxidation state, but often the reduced +5 oxidation state is observed. The number of charge-compensating cations required in a structure therefore depends on the degree to which the Mo atoms are reduced. Because of the possibility of electron delocalization in such mixed-valence systems, these structures often exhibit interesting properties, which make them potentially useful in nanoscale electronic and magnetic materials. In order for these structures to be useful as functional nanomaterials, one must gain control over cluster arrangement in the molecular assemblies. The number, size, and charge of the constituent counter-cations, as well as the nature of other structure-building moieties, dictate the overall molecular and structural arrangement of these cluster compounds. Consequently, it is

critically important that all of these factors be well-controlled by careful selection of cations, and by following appropriate synthetic routes to generate systems of interest. The incorporation of a variety of cations in the formation of molybdate compounds has been achieved. This includes the incorporation of organic cations originating from ionic liquids to synthesize molybdates in either crystal or simply solid form.⁷³⁻⁷⁶ However, in these referenced cases, which were discovered using SciFinder, the synthesis was carried out with intermediates which already possessed the desired anionic cluster, coordinated by proton counter-cations.

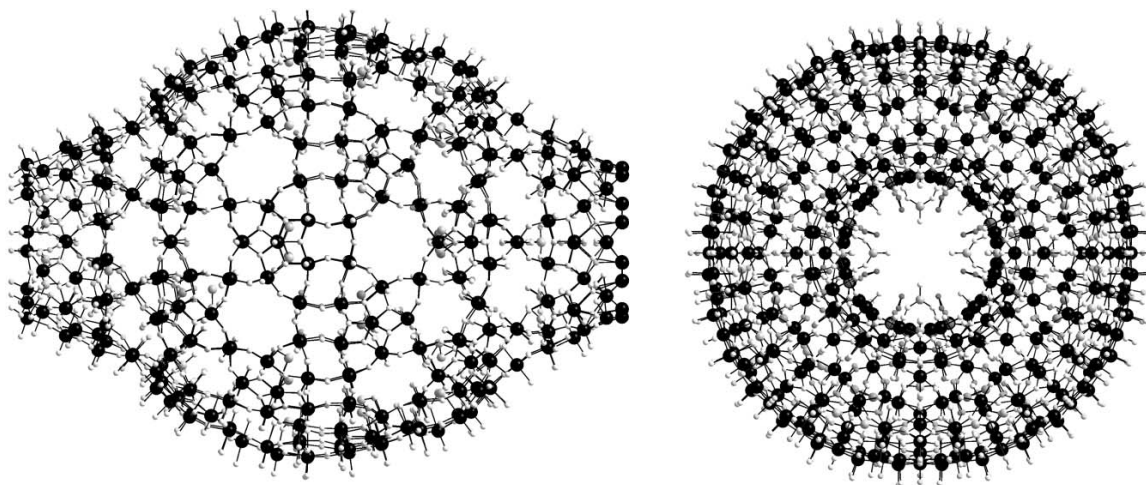


Fig. 1-3. The structure of the $\{\text{Mo}_{368}\}$ 'lemon' cluster. The side view is shown (LHS) and the top view is also shown (RHS).⁶¹

Before 2003, at which time Samantha Levine conducted her studies (see Chapter 1), no one had reported using RTILs to synthesize polyoxomolybdate compounds in crystal form by constructing the molybdate clusters in the ionic liquid from simple molybdate salts, while at the same time incorporating the cation of the ionic liquid to achieve charge balance. In June of 2003, Dr. Greenblatt's group of our chemistry department reported the ionothermal synthesis of $(\text{emim})_4[\text{Mo}_8\text{O}_{26}]$ at the 36th Middle Atlantic Regional Meeting of the ACS.⁷⁷

This compound was synthesized in molten 1-ethyl-3-methyl-imidazolium chloride using the simple molybdate salt $(\text{NH}_4)_6\text{Mo}_7\text{O}_{24}\cdot 4\text{H}_2\text{O}$. This appears to be the first report of a polyoxomolybdate synthesized using the general synthetic strategy outlined above. In 2008, the ionothermal synthesis of this same structure from $(\text{emim})[\text{BF}_4]$ (a liquid at RT) using $\text{Na}_2\text{MoO}_4\cdot 2\text{H}_2\text{O}$ was reported.⁷⁸ Finally, in 2010 the ionothermal synthesis of $(\text{emim})_4[\text{SiMo}_{12}\text{O}_{40}]$ from $(\text{emim})[\text{Br}]$ (a solid at RT) using $\text{Na}_2\text{MoO}_4\cdot 2\text{H}_2\text{O}$, $\text{Na}_2\text{SiO}_3\cdot 9\text{H}_2\text{O}$, and glacial acetic acid was reported.⁷⁹ In this paragraph, the first and third reports were discovered using SciFinder, and the second report was found using the International Union of Crystallography's online search engine.

This thesis details the efforts that members of our research group, myself included, have made in this area. The title polyoxomolybdates appear to be the first to be synthesized from $(\text{bmim})[\text{BF}_4]$ using simple molybdate salts. Compounds **1** and **2** appear to have never been reported. Compounds with the formula of compound **3** have been reported. However, only crystal data for one of these compounds seems to be available, and the crystal system and space group of this compound do not match those of compound **3**. Therefore, technically speaking compound **3** appears to be a new compound as well. Even if compound **3** has already been reported, we were able to synthesize it in what may be a new way (i.e. by not using intermediates). Compound **3** also appears to be the first polyoxomolybdate synthesized using our approach which also possesses catalytic properties.

References

- (1) Wasserscheid, P.; Keim, W. *Angew. Chem., Int. Ed.* 2000, *39*, 3773-3789.
- (2) Larionova, J.; Guari, Y.; Sayegh, H.; Guerin, C. *Inorg. Chim. Acta* 2007, *360*, 3829-3836.
- (3) Sugden, S.; Wilkins, H. *J. Chem. Soc.* 1929, 1291-1298.
- (4) Wallach, O. *Chem. Ber.* 1884, *16*, 535.
- (5) Seddon, K. R. In *Molten Salt Chemistry*; Mamantov, G., Marassi, R., Eds.; Reidel Publishing Co.: Dordrecht, The Netherlands, 1987; pp 365.
- (6) Wilkes, J. S.; Levisky, J. A.; Wilson, R. A.; Hussey, C. L. *Inorg. Chem.* 1982, *21*, 1263-1264.
- (7) Hussey, C. L. In *Advances in Molten Salts Chemistry*; Mamantov, G., Mamantov, C., Eds.; Elsevier: New York, 1983; Vol. 5, pp 185-230.
- (8) Dieter, K. M.; Dymek, C. J.; Heimer, N. E.; Rovang, J. W.; Wilkes, J. S. *J. Am. Chem. Soc.* 1988, *110*, 2722-2726.
- (9) Wilkes, J. S.; Zaworotko, M. J. *J. Chem. Soc., Chem. Commun.* 1992, 965-967.
- (10) Li, Z.; Jia, Z.; Luan, Y.; Mu, T. *Current Opinion in Solid State and Materials Science* 2008, *12*, 1-8.
- (11) Reichert, W. M.; Holbrey, J. D.; Vigour, K. B.; Morgan, T. D.; Broker, G. A.; Rogers, R. D. *Chem. Commun.* 2006, 4767-4779.
- (12) Forsyth, S. A.; Pringle, J. M.; MacFarlane, D. R. *Aust. J. Chem.* 2004, *57*, 113-119.
- (13) Hussey, C. L. *Pure Appl. Chem.* 1988, *60*, 1763-1772.
- (14) Seddon, K. R. *J. Chem. Technol. Biotechnol.* 1997, *68*, 351-356.
- (15) Huddleston, J. G.; Willauer, H. D.; Swatloski, R. P.; Visser, A. E.; Rogers, R. D. *Chem. Commun.* 1998, 1765-1766.
- (16) Greaves, T. L.; Drummond, C. J. *Chem. Soc. Rev.* 2008, *37*, 1709-1726.
- (17) van Rantwijk, F.; Sheldon, R. A. *Chem. Rev.* 2007, *107*, 2757-2785.
- (18) Parvulescu, V. I.; Hardacre, C. *Chem. Rev.* 2007, *107*, 2615-2665.
- (19) Muzart, J. *Adv. Synth. Catal.* 2006, *348*, 275-295.
- (20) Jain, N.; Kumar, A.; Chauhan, S.; Chauhan, S. M. S. *Tetrahedron* 2005, *61*, 1015-1060.
- (21) Dupont, J.; de Souza, R. F.; Suarez, P. A. Z. *Chem. Rev.* 2002, *102*, 3667-3691.
- (22) Welton, T. *Chem. Rev.* 1999, *99*, 2071-2083.
- (23) Rogers, R. D.; Seddon, K. R. *Science* 2003, *302*, 792-793.
- (24) Xu, W.; Angell, C. A. *Science* 2003, *302*, 422-425.
- (25) Kubo, W.; Kitamura, T.; Hanabusa, K.; Wada, Y.; Yanagida, S. *Chem. Commun.* 2002, 374-375.
- (26) Wang, P.; Zakeeruddin, S. M.; Moser, J. E.; Gratzel, M. *J. Phys. Chem. B* 2003, *107*, 13280-13285.
- (27) Wang, P.; Zakeeruddin, S. M.; Humphry-Baker, R.; Gratzel, M. *Chem. Mater.* 2004, *16*, 2694-2696.
- (28) Wang, P.; Wenger, B.; Humphry-Baker, R.; Moser, J. E.; Teuscher, J.; Kantelehner, W.; Mezger, J.; Stoyanov, E. V.; Zakeeruddin, S. M.; Gratzel, M. *J. Am. Chem. Soc.* 2005, *127*, 6850-6856.
- (29) Kuang, D. B.; Ito, S.; Wenger, B.; Klein, C.; Moser, J. E.; Humphry-Baker, R.; Zakeeruddin, S. M.; Gratzel, M. *J. Am. Chem. Soc.* 2006, *128*, 4146-4154.
- (30) Kuang, D. B.; Wang, P.; Ito, S.; Zakeeruddin, S. M.; Gratzel, M. *J. Am. Chem. Soc.* 2006, *128*, 7732-7733.
- (31) Yang, Z.; Pan, W. B. *Enzyme Microb. Technol.* 2005, *37*, 19-28.

- (32) Del Popolo, M. G.; Voth, G. A. *J. Phys. Chem. B* 2004, *108*, 1744-1752.
- (33) Parnham, E. R.; Morris, R. E. *Acc. Chem. Res.* 2007, *40*, 1005-1013.
- (34) Jin, K.; Huang, X. Y.; Pang, L.; Li, J.; Appel, A.; Wherland, S. *Chem. Commun.* 2002, 2872-2873.
- (35) Dybtsev, D. N.; Chun, H.; Kim, K. *Chem. Commun.* 2004, 1594-1595.
- (36) Lin, Z. J.; Wragg, D. S.; Warren, J. E.; Morris, R. E. *J. Am. Chem. Soc.* 2007, *129*, 10334-10335.
- (37) Xu, L.; Choi, E. Y.; Kwon, Y. U. *Inorg. Chem.* 2008, *47*, 1907-1909.
- (38) Pedireddi, V. R.; Shimpi, M. R.; Yakhmi, J. V. *Macromol. Symp.* 2006, *241*, 83-87.
- (39) Xu, L.; Choi, E. Y.; Kwon, Y. U. *Inorg. Chem.* 2007, *46*, 10670-10680.
- (40) Lin, Z. J.; Wragg, D. S.; Morris, R. E. *Chem. Commun.* 2006, 2021-2023.
- (41) Lin, Z. J.; Slawin, A. M. Z.; Morris, R. E. *J. Am. Chem. Soc.* 2007, *129*, 4880-4881.
- (42) Jacob, D. S.; Kahlenberg, V.; Wurst, K.; Solovyov, L. A.; Felner, I.; Shimon, L.; Gottlieb, H. E.; Gedanken, A. *Eur. J. Inorg. Chem.* 2005, 522-528.
- (43) Liao, J. H.; Wu, P. C.; Bai, Y. H. *Inorg. Chem. Commun.* 2005, *8*, 390-392.
- (44) Liao, J. H.; Wu, P. C.; Huang, W. C. *Cryst. Growth Des.* 2006, *6*, 1062-1063.
- (45) Sheu, C. Y.; Lee, S. F.; Lii, K. H. *Inorg. Chem.* 2006, *45*, 1891-1893.
- (46) Cooper, E. R.; Andrews, C. D.; Wheatley, P. S.; Webb, P. B.; Wormald, P.; Morris, R. E. *Nature* 2004, *430*, 1012-1016.
- (47) Parnham, E. R.; Wheatley, P. S.; Morris, R. E. *Chem. Commun.* 2006, 380-382.
- (48) Parnham, E. R.; Morris, R. E. *J. Am. Chem. Soc.* 2006, *128*, 2204-2205.
- (49) Wang, L.; Xu, Y. P.; Wei, Y.; Duan, J. C.; Chen, A. B.; Wang, B. C.; Ma, H. J.; Tian, Z. J.; Lin, L. W. *J. Am. Chem. Soc.* 2006, *128*, 7432-7433.
- (50) Clavel, G.; Larionova, J.; Guari, Y.; Guerin, C. *Chem.--Eur. J.* 2006, *12*, 3798-3804.
- (51) Wei, G. T.; Yang, Z. S.; Lee, C. Y.; Yang, H. Y.; Wang, C. R. C. *J. Am. Chem. Soc.* 2004, *126*, 5036-5037.
- (52) Itoh, H.; Naka, K.; Chujo, Y. *J. Am. Chem. Soc.* 2004, *126*, 3026-3027.
- (53) Kim, K. S.; Demberelnyamba, D.; Lee, H. *Langmuir* 2004, *20*, 556-560.
- (54) Dupont, J.; Fonseca, G. S.; Umpierre, A. P.; Fichtner, P. F. P.; Teixeira, S. R. *J. Am. Chem. Soc.* 2002, *124*, 4228-4229.
- (55) Scheeren, C. W.; Machado, G.; Dupont, J.; Fichtner, P. F. P.; Teixeira, S. R. *Inorg. Chem.* 2003, *42*, 4738-4742.
- (56) Huang, J.; Jiang, T.; Han, B. X.; Gao, H. X.; Chang, Y. H.; Zhao, G. Y.; Wu, W. Z. *Chem. Commun.* 2003, 1654-1655.
- (57) Calo, V.; Nacci, A.; Monopoli, A.; Laera, S.; Cioffi, N. *J. Org. Chem.* 2003, *68*, 2929-2933.
- (58) Deshmukh, R. R.; Rajagopal, R.; Srinivasan, K. V. *Chem. Commun.* 2001, 1544-1545.
- (59) Zhu, Y. J.; Wang, W. W.; Qi, R. J.; Hu, X. L. *Angew. Chem., Int. Ed.* 2004, *43*, 1410-1414.
- (60) Nakashima, T.; Kimizuka, N. *J. Am. Chem. Soc.* 2003, *125*, 6386-6387.
- (61) Long, D. L.; Burkholder, E.; Cronin, L. *Chem. Soc. Rev.* 2007, *36*, 105-121.
- (62) Muller, A.; Peters, F.; Pope, M. T.; Gatteschi, D. *Chem. Rev.* 1998, *98*, 239-271.
- (63) Long, D. L.; Cronin, L. *Chem.--Eur. J.* 2006, *12*, 3699-3706.
- (64) Borrás-Almenar, J. J.; Coronado, E.; Muller, A.; Pope, M. *Polyoxometalate Molecular Science*; Kluwer Academic Publishers: London, 2001.
- (65) Pope, M.; Muller, A. *Polyoxometalate Chemistry From Topology via Self-Assembly to Applications*; Kluwer Academic Publishers: London, 2001.

- (66) Yamase, T.; Pope, M. *Polyoxometalate Chemistry for Nano-Composite Design*; Kluwer Academic Publishers: New York, 2002.
- (67) Cronin, L. In *Comprehensive Coordination Chemistry II*; McCleverty, J. A., Meyer, T. J., Eds.; Elsevier: Amsterdam, 2004; Vol. 7, pp 1–56.
- (68) Muller, A.; Kogerler, P.; Kuhlmann, C. *Chem. Commun.* 1999, 1347-1358.
- (69) Muller, A.; Kogerler, P.; Dress, A. W. M. *Coord. Chem. Rev.* 2001, 222, 193-218.
- (70) Muller, A.; Serain, C. *Acc. Chem. Res.* 2000, 33, 2-10.
- (71) Muller, A.; Roy, S. *Coord. Chem. Rev.* 2003, 245, 153-166.
- (72) Akutagawa, T.; Endo, D.; Noro, S. I.; Cronin, L.; Nakamura, T. *Coord. Chem. Rev.* 2007, 251, 2547-2561.
- (73) Rao, G. R.; Rajkumar, T; Varghese, B. *Solid State Sci.* 2009, 11, 36-42.
- (74) Kim, J. D. Proton conductors showing phase change at high temperatures, method for their manufacture, and fuel cells with the conductors. Japan Patent JP 2009016156, January 22, 2009.
- (75) Karthik, G. Synthesis of 1-butyl-3-methylimidazolium phosphomolydate. India Patent IN 2007DE02014, April 24, 2009.
- (76) Ammam, M.; Fransaer, J. *J. Electrochem. Soc.* 2011, 158, A14-A21.
- (77) Whaley, L.; Bune, R.O.; Emge, T.; Greenblatt, M. *Abstracts*, 36th Middle Atlantic Regional Meeting of the American Chemical Society, Princeton, NJ, June 8-11, 2003; American Chemical Society: Washington, DC, 2003; 69EBDT.
- (78) Lin, S.; Chen, W.; Zhang, Z.; Liu, W.; Wang, E. *Acta Crystallogr., Sect. E: Struct. Rep. Online* 2008, 64, m954.
- (79) Lin, S.; Liu, W.; Li, Y.; Wu, Q.; Wang, E.; Zhang, Z. *Dalton Trans.* 2010, 39, 1740-1744.

CHAPTER 1

Historical polyoxomolybdates

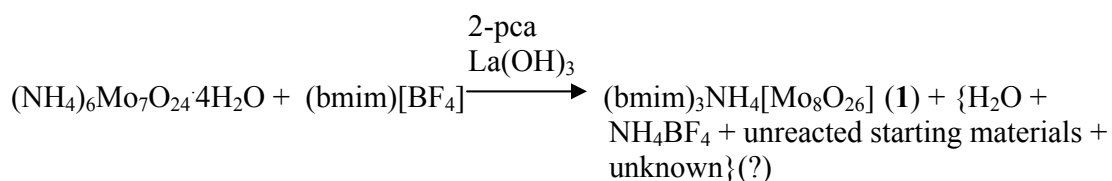
Work in our lab pertaining to the synthesis of coordination compounds using ionic liquids as solvents began in 2003. The ionic liquid (bmim)[BF₄] was selected for use as a solvent in initial trial experiments. Two structures were successfully synthesized, and both were polyoxomolybdate compounds. Soon after I began my graduate research during the summer of 2009, my first project was to reproduce these two compounds, before moving on to other ionic liquid-based reactions. The following two chapters will illustrate a portion of the work that has been done in this context.

(bmim)₃NH₄[Mo₈O₂₆] (1)

Synthesis and Crystal Structure

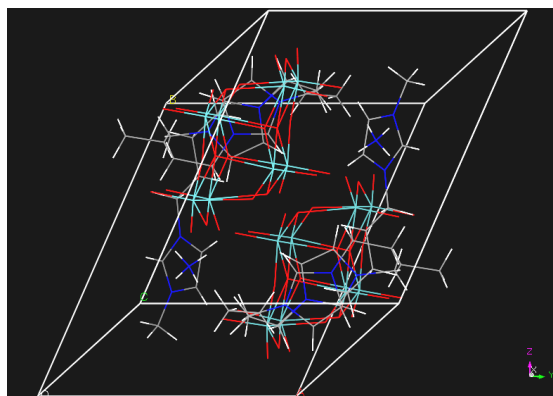
Large colorless crystals of compound **1** with the formula (bmim)₃NH₄[Mo₈O₂₆] (**1**) were first obtained via the following ionothermal bomb reaction at 140 °C for 6 days (Scheme 2-1).

Scheme 2-1

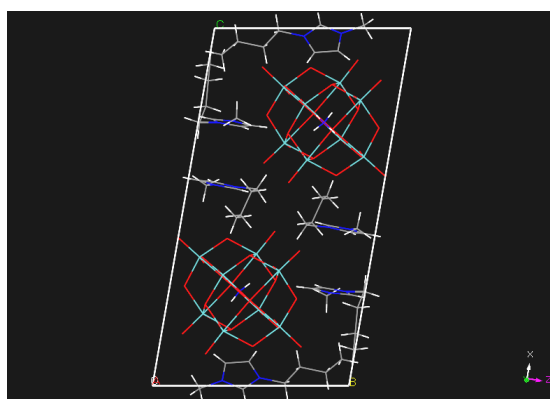


The single crystal x-ray diffraction analysis indicated that the compound crystallized in the triclinic space group P-1. It was originally believed that the crystallographic asymmetric unit contained one octamolybdate cluster (8 Mo, 26 O), three bmim molecules, and one H₃O⁺ molecule. However, upon further analysis, it was decided that the asymmetric unit contained one NH₄⁺ molecule instead of a H₃O⁺ molecule. The unit cell, which contains a total of two

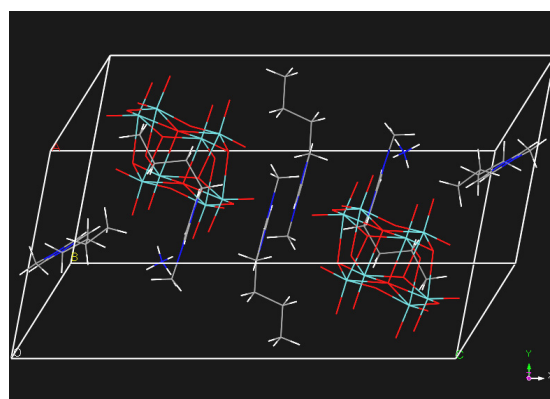
octamolybdate clusters (both carrying a 4- charge), six bmim molecules (each carrying a +1 charge), and two NH_4^+ molecules, is generated by applying inversion symmetry to the asymmetric unit. All ions are found on general positions. Three different views of the unit cell are shown in Figure 2-1 below.



(a)



(b)



(c)

Fig. 2-1. View of the unit cell of **1** projected along the (a) x axis (b) y axis and (c) z axis. Disorder in the imidazolium cations is not shown for clarity. Color explanation: Light blue, Mo; Dark blue, N; Red, O; Grey, C; White, H.

As of 2005, 8 isomers of octamolybdates had been identified, which “...differ in the number, type, and fusion mode of the molybdenum polyhedron.”¹ Based on a description presented in this same reference, and the images found in Figure 2-1 above, the

octamolybdates in this structure are of the β form, which "... is composed of an array of eight edge-sharing $\{\text{MoO}_6\}$ octahedra."¹ The Mo–O distances range from 1.6966(14)–2.5181(13) Å. This overall range is comparable to that of other 4- charge β -octamolybdate structures, including one which contains ionic liquid cations.^{2,3} Upon closer inspection of the asymmetric unit, we find that the 14 Mo–O bonds involving 14 terminal oxygens range from 1.6966(14)–1.7185(14) Å, the 12 Mo–O bonds involving six doubly bridged oxygens range from 1.7506(13)–2.2835(13) Å, the 12 Mo–O bonds involving four triply bridged oxygens range from 1.9366(13)–2.3154(13) Å, and the 10 Mo–O bonds involving two quintuply bridged oxygens range from 2.1269(13)–2.5181(13) Å. When we compare these ranges with those observed by Gong et al,⁴ we notice that our doubly bridged range is significantly wider on the high end of the range. However, the ranges given for compound **1** do seem to correlate well with the selected bond distances provided by Duraisamy et al.⁵ As for all bonds, the bond distances discussed above, as well as in other portions of this thesis, are inversely proportional to bond strength. Two types of hydrogen bonds are present in this structure. The first is of the type N–H---O, due to the presence of the NH_4^+ cation found in the structure. We find that each hydrogen atom in the cation has a hydrogen bond with a unique terminal oxygen atom of an octamolybdate cluster, so that two clusters in separate unit cells are connected by one NH_4^+ cation. When this hydrogen bonding scheme is extended to multiple unit cells, chains of alternating NH_4^+ cations and octamolybdate anions are observed. These chains run along the y axis. The N---O distances range from 2.825(2)–3.022(2) Å. The other hydrogen bonds are of the type C–H---O. These bonds (10 in total) are present due to interactions between imidazolium cations and octamolybdate clusters. One of the interactions involves disordered atoms (disorder, which is caused by rotational isomerism, is present in one out of the three imidazolium cations in the asymmetric

unit, specifically in the atoms of the butyl group). For these 10 interactions, the C---O distances range from 3.017(2)–3.356(3) Å.

The three inter-ionic O---O distances in this compound range from 2.868–4.014 Å. The shortest N---N distance between two imidazolium cations is 3.639 Å. The shortest distance between the N atom of an NH_4^+ cation and the N atom of an imidazolium cation is 5.068 Å. O–Mo–O bond angles range from 68.84(4)–175.20(6)°. This range in bond angles agrees well with literature reports.^{2,4} The selected bond angles given in reference 5 also fall within the range given for compound **1**.

A summary of the crystal data for **1** is provided in Table 2-1 below.

Table 2-1 Crystal Data for (bmim)₃NH₄[Mo₈O₂₆]

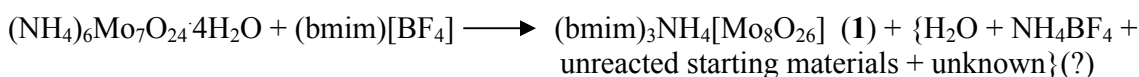
1	
Molecular formula	(bmim) ₃ NH ₄ [Mo ₈ O ₂₆]
FW	1619.22
Space group	P-1
a (Å)	9.9473(5)
b (Å)	12.2700(8)
c (Å)	21.0254(10)
α	76.700(1)
β	79.222(1)
γ	66.301(1)
V(Å ³)	2273.9(2)
Z	2
T, K	100(2)
λ , Å	0.71073
ρ_{calc} , gcm ⁻³	2.365
μ (mm ⁻¹)	2.224
$R[F^2 > 2\sigma(F^2)]$	0.0372
$wR(F^2)$	0.0662

$$R = \frac{\sum ||F_o| - |F_c||}{\sum |F_o|}, wR = \sqrt{\frac{\sum [w(F_o^2 - F_c^2)^2]}{\sum w(F_o^2)^2}}, w = 1/[\sigma^2(F_o^2) + (0.0200P)^2 + 4.0000P],$$

$$P = (F_o^2 + 2F_c^2)/3$$

Even before further refinement, it was noticed that neither $\text{La}(\text{OH})_3$ nor 2-pca incorporated themselves into the structure. Therefore, my attempts to reproduce this structure did not make use of these reagents. My best results were achieved via the following ionothermal glass vial reaction at 120 °C for 7 days (Scheme 2-2).

Scheme 2-2



Characterization

The PXRD pattern and TGA plot of **1** (both obtained using pure material from the reaction referenced in Scheme 2-2) are shown in Fig. 2-2 below.

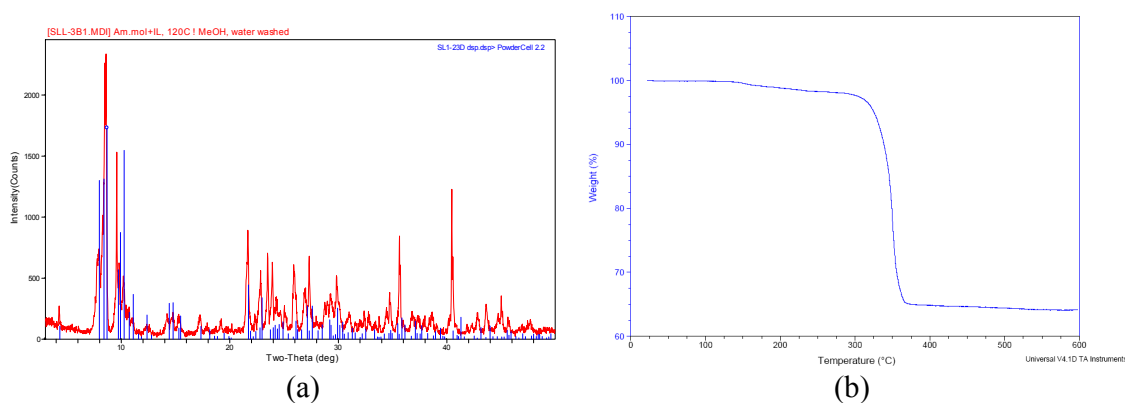


Fig. 2-2. (a) The PXRD pattern for **1**, where the red trace is the pattern generated from material obtained from the Scheme 2-2 reaction, and the blue trace is the simulated pattern generated from material from the Scheme 2-1 reaction (b) The TGA plot for **1** (approx. 5 mg of **1** heated at a rate of 5 °C/min)

As shown in Figure 2-2a, the simulated and experimental PXRD patterns match quite well. When dealing with polyoxomolybdate compounds, we are generally most concerned with the most prominent peaks which typically exist in the 2θ range of about 8–10, and in this case we find that these peaks match quite well. As shown in Figure 2-2b, compound **1** is

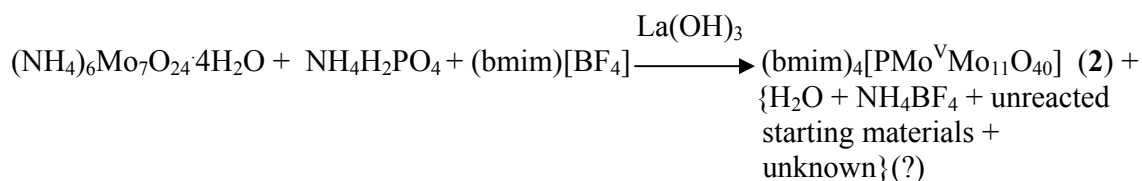
thermally stable to approximately 125 °C. It loses weight until about 360 °C. The total weight loss is 35.87%.

(bmim)₄[PMo^VMo₁₁O₄₀] (2)

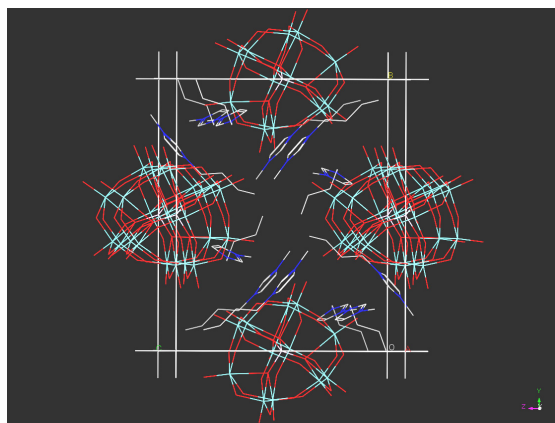
Synthesis and Crystal Structure

Blue block crystals of compound **2** with the formula (bmim)₄[PMo^VMo₁₁O₄₀] were first obtained via the following ionothermal bomb reaction at 135 °C for 6 days (Scheme 2-3).

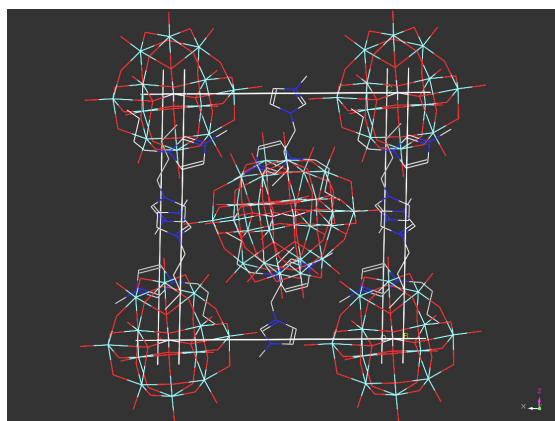
Scheme 2-3



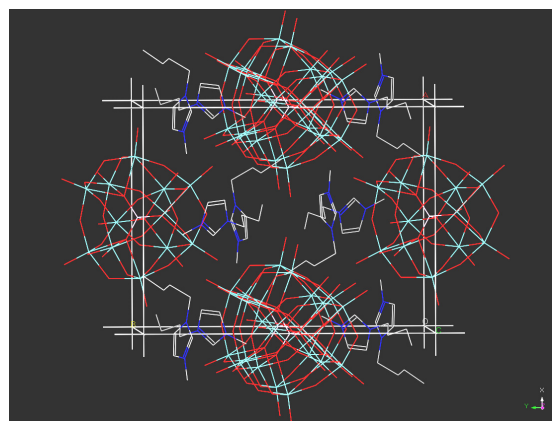
The single crystal x-ray diffraction analysis indicated that the compound crystallized in the monoclinic space group P2₁/n. The crystallographic asymmetric unit contains one Keggin anionic cluster (1 P, 12 Mo, 40 O) and four bmim molecules. The unit cell, which contains a total of two mixed valence one-electron reduced Keggin clusters (each carrying a 4- charge) and eight bmim molecules (each carrying a +1 charge), is generated by applying to the asymmetric unit 2-fold screw symmetry along the b axis and an n glide plane perpendicular to the b axis. Three different views of the unit cell are shown in Figure 2-3 below. Because the Keggin clusters are reduced by one electron, compound **2** can be classified as a charge transfer salt, in which the bmim cations act as electron donors and the Keggin anions act as electron acceptors.⁶



(a)



(b)



(c)

Fig. 2-3. View of the unit cell of **2** projected approximately along the (a) x axis (b) y axis and (c) z axis. Disorder in the anionic Keggin clusters is not shown for clarity. Color explanation: Light blue, Mo; Dark blue, N; Purple, P; Red, O; Grey, C.

As described in the article⁷ which is discussed in Chapter 2, the Keggin anions are constructed from

“... four M_3O_{13} groups ($M = \text{Mo}, \text{W}$) surrounding a central heteroatom in a tetrahedral cavity. Each M_3O_{13} group is formed by three octahedral sharing edges and having a common oxygen atom which is also shared with the central heteroatom.”

In our case, M represents an Mo atom, and the heteroatom is P. Further, we know that the Keggin anions are of the α form⁸ because the “... four corner-sharing ... triad clusters ... are arrayed around the center ... tetrahedron in an ideal C_s symmetry. The central ... atom lies at

a site with $\bar{4}$ symmetry.” This statement should be qualified in our case, because our anions have approximate tetrahedral symmetry. We know we do not have Keggin anions in the β form⁹ for example because “the β -Keggin type structure derives from the α -Keggin by a rotation of 60° of one of the Mo_3O_{13} units...” The Mo–O distances in **2** range from 1.61(3)–2.456(7) Å. A closer inspection of the asymmetric unit reveals that the 12 Mo–O bonds involving 12 terminal oxygens range from 1.61(3)–1.74(2) Å, the 48 Mo–O bonds involving 24 doubly bridged oxygens range from 1.830(19)–1.988(16) Å, and the 12 Mo–O bonds involving four phosphate oxygens range from 2.405(11)–2.456(7) Å. The four P–O bonds range from 1.477(4)–1.616(5) Å. These ranges for specific types of bonds generally agree with reported values for 4- charge phosphorus-containing α -Keggin molybdate clusters.¹⁰⁻¹² References 10 and 11 only provide Mo–O bond distances. All of the Mo and O atoms in **2** have an occupancy of 0.5, whereas the central phosphorus atom has an occupancy of 1. This is due to the fact that the anions are located on inversion centers. The atoms of the cations all have an occupancy of 1. Mo–O–Mo bond angles involving phosphate oxygen atoms range from 88.0(3)–90.2(4) $^\circ$, while Mo–O–Mo bond angles involving bridging oxygen atoms range from 124.1(5)–127.1(5) $^\circ$ and from 148.1(5)–152.6(6) $^\circ$. These bond angles generally agree with angles presented in reference 12, but it should be noted that the angles quoted in reference 12 apply to a 3- charge structure. In reference 12, the authors explain that:

“The bond angles of Mo–O_c–Mo are in the range of 88.76(12)–89.08(12) $^\circ$, and those of Mo–O_b–Mo fall into two groups: 124.9(2)–126.2(2) $^\circ$ in a Mo_3O_{13} triplet and 151.5(2)–152.3(2) $^\circ$ between two Mo_3O_{13} triplets.”

The tetrahedral O–P–O angles range from 104.3(2)–114.9(3) $^\circ$. The ideal tetrahedral angle is 109.5 $^\circ$. Therefore, there is some departure from ideality in the central PO_4 group.

The distances between the P atoms of two different Keggin clusters in the unit cell

range from 12.824–19.739 Å. The shortest N---N distance between two different imidazolium cations in the unit cell is 5.028 Å. The nine unique inter-ionic O---O distances in this structure range from 3.0513–3.4306 Å. In addition, no hydrogen bonding is present in compound **2**.

A summary of the crystal data for **2** is provided in Table 2-2 below.

Table 2-2 Crystal Data for
(bmim)₄[PMo^VMo₁₁O₄₀]

2	
Molecular formula	(bmim) ₄ [PMo ^V Mo ₁₁ O ₄₀]
FW	2379.13
Space group	<i>P2₁/n</i>
a (Å)	13.159(3)
b (Å)	16.952(3)
c (Å)	14.383(3)
α	90.00
β	91.45(3)
γ	90.00
V(Å ³)	3207.41(11)
Z	2
T, K	293(2)
λ, Å	0.71073
ρ _{calc} , gcm ⁻³	2.463
μ (mm ⁻¹)	2.386
R[F ² > 2σ(F ²)]	0.0278
wR(F ²)	0.0659

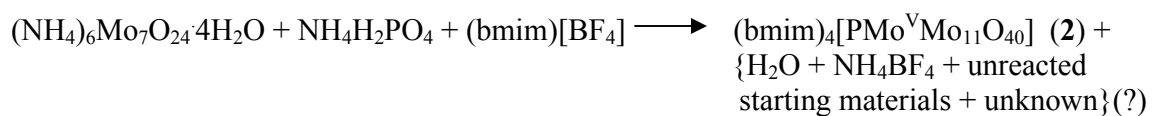
$$R = \frac{\sum ||F_o| - |F_c||}{\sum |F_o|}, wR = \sqrt{\frac{\sum [w(F_o^2 - F_c^2)^2]}{\sum w(F_o^2)^2}}, w = 1/[\sigma^2(F_o^2) + (0.0300P)^2 + 5.0000P],$$

$$P = (F_o^2 + 2F_c^2)/3$$

It was noticed that La(OH)₃ did not incorporate itself into the structure. Therefore, attempts to reproduce this compound did not make use of this reagent. Moothetty

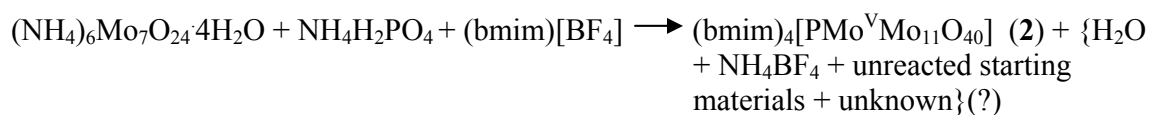
Padmanabhan was able to reproduce this compound via the following ionothermal glass vial reaction at 120 °C for four days (Scheme 2-4).

Scheme 2-4



My best results were obtained via the following ionothermal bomb reaction at 140 °C for seven days (Scheme 2-5).

Scheme 2-5



At first glance, the above two schemes look very similar. However, if we refer to the experimental section, we see that the two reactions are significantly different regarding the actual reaction conditions.

Characterization

PXRD patterns as well as a TGA plot for **2** are shown in Fig. 2-4 below.

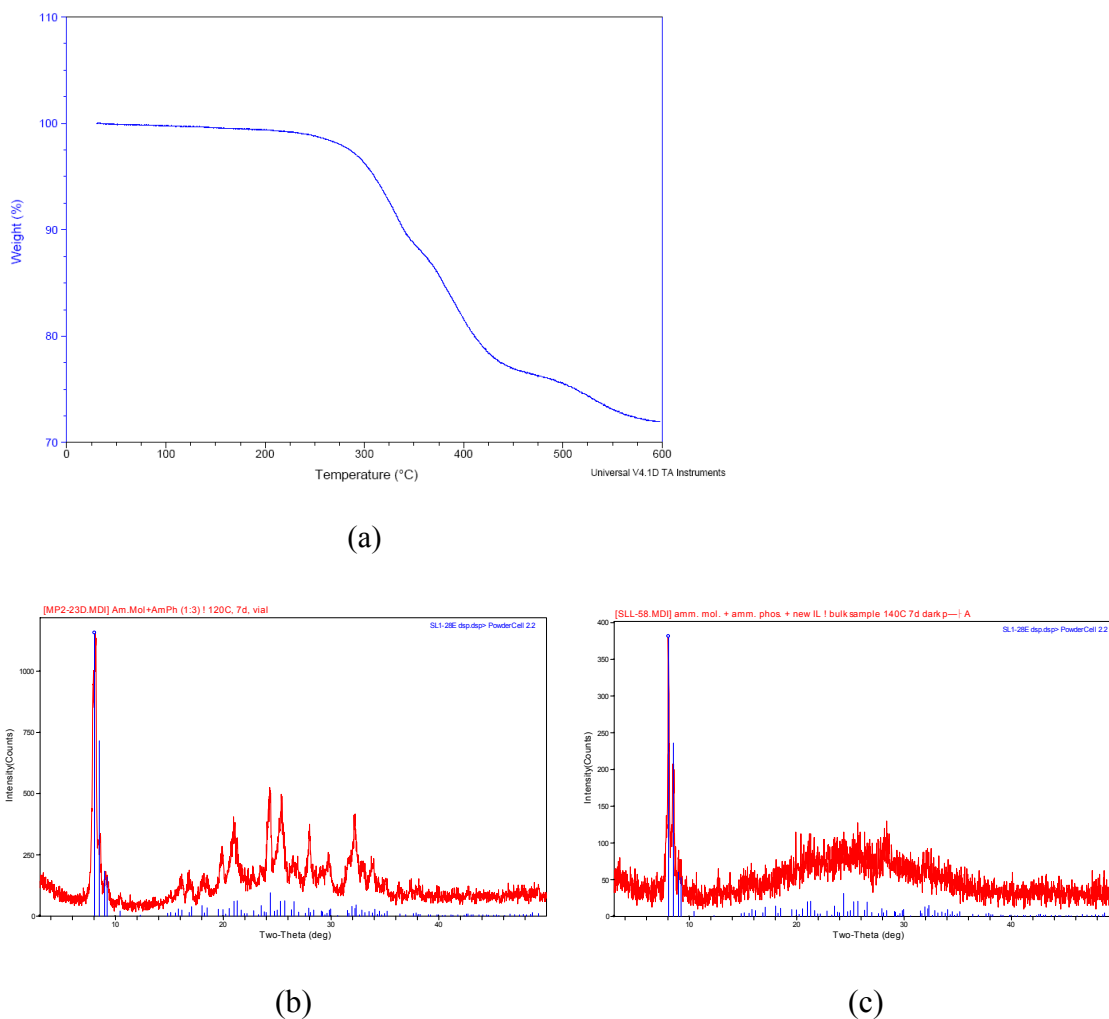


Fig. 2-4. (a) The TGA plot for **2**, taken with pure material from the Scheme 2-4 reaction (approx. 3 mg of **2** heated at a rate of 5 °C/min) (b) A PXRD pattern for **2**, where the red trace is the pattern generated from pure material obtained from the Scheme 2-4 reaction, and the blue trace is the simulated pattern generated from material from the Scheme 2-3 reaction (c) A PXRD pattern for **2**, where the red trace is the pattern generated from impure material obtained from the Scheme 2-5 reaction, and the blue trace is the simulated pattern generated from material from the Scheme 2-3 reaction.

As shown in Figure 2-4a, compound **2** is thermally stable up to 250 °C. As shown in Figures 2-4b and c, simulated and experimental PXRD patterns generally match, especially in

the 2θ range of about 8–10. The experimental pattern in Figure 2-4b is of higher quality, likely because more sample was used for data collection, and also because the sample was indeed more pure.

Summary

This chapter discussed the synthesis of two polyoxomolybdate compounds via ionothermal synthesis. They were first synthesized as the result of a combinatorial approach, and were later reproduced in a more rational manner. Both syntheses involved the usage of ammonium molybdate and the ionic liquid (bmim)[BF₄]. The presence of ammonium phosphate in the synthesis of **2** resulted in the formation of a phosphorus-containing Keggin-based structure rather than a simpler octamolybdate-based structure. In **1**, an NH₄⁺ cation is incorporated to help balance the negatively charged octamolybdate, whereas in **2**, only imidazolium cations are present. Hydrogen-bonding is present in **1**, but not in **2**. In **1**, we find that the octamolybdate clusters are not disordered, but that disorder is present in one out of three imidazolium cations. In **2**, disorder is present in the Keggin clusters, but not in the imidazolium cations.

In chapter 2, a technically-new polyoxomolybdate which has also been synthesized in a novel manner will be discussed. The discussion will include some interesting synthetic observations, as well as catalytic data.

References

- (1) Sun, C.; Wang, E.; An, H.; Xiao, D.; Xu, L. *Transition Met. Chem.* 2005, 30, 873-878.
- (2) Lin, S.; Chen, W.; Zhang, Z.; Liu, W.; Wang, E. *Acta Crystallogr., Sect. E: Struct. Rep. Online* 2008, 64, m954.
- (3) Wang, X.; Chen, B.; Liu, G.; Zhao, H.; Lin, H.; Hu, H. *Solid State Sci.* 2009, 11, 61-67.
- (4) Gong, Y.; Hu, C.W.; Xia, Z. N. *J. Mol. Struct.* 2007, 837, 48-57.
- (5) Duraisamy, T.; Ramanan, A.; Vittal, J. J. *J. Mater. Chem.* 1999, 9, 763-767.
- (6) Liu, X.; Xue, G.; Hu, H.; Gao, Q.; Fu, F.; Wang, J. *J. Mol. Struct.* 2006, 787, 101-105.
- (7) Lu, Y.; Xu, Y.; Wang, E.; Li, Y.; Wang, L.; Hu, C.; Xu, L. *J. Solid State Chem.* 2004, 177, 2210-2215.
- (8) Wang, X.; Qin, C.; Wang, E.; Su, Z. *Chem. Commun.* 2007, 4245-4247.
- (9) Dolbecq, A.; Cadot, E.; Eisner, D.; Sécheresse, F. *Inorg. Chem.* 1999, 38, 4217-4223.
- (10) Kurmoo, M.; Bonamico, M.; Bellitto, C.; Fares, V.; Federici, F.; Guionneau, P.; Ducasse, L.; Kitagawa, H.; Day, P. *Adv. Mater.* 1998, 10, 545-550.
- (11) Bellitto, C.; Bonamico, M.; Fares, V.; Federici, F.; Righini, G. *Chem. Mater.* 1995, 7, 1475-1484.
- (12) Zhai, Q.; Wu, X.; Chen, S.; Zhao, Z.; Lu, C. *Inorg. Chem.* 2007, 46, 5046-5058.

CHAPTER 2

A new polyoxomolybdate

In 2004, two interesting isostructural Keggin-based molecules which form 1D chains, $[\text{H}_2\text{bpy}]_2[\text{Hbpy}][\text{PCuMo}_{11}\text{O}_{39}]\cdot\text{H}_2\text{O}$ and $[\text{H}_2\text{bpy}]_2[\text{Hbpy}][\text{PZnMo}_{11}\text{O}_{39}]\cdot 2.75\text{H}_2\text{O}$, were reported.¹ One of the structures had a copper atom in place of one of the molybdenum atoms, whereas the other structure had a zinc atom. A depiction of the copper compound, which is referred to in the journal article as compound **1**, is provided in Figure 3-1 below. In the article, water was used as the solvent, and 4,4'-bipyridine (which was protonated either once or twice during the reaction) was used as the organic ligand. These results inspired the eventual synthesis of compound **3**. The original intent was to synthesize a Keggin-based structure, in which one molybdenum atom was replaced by a copper atom, but to incorporate the organic cation of $(\text{bmim})[\text{BF}_4]$ into the structure rather than protonated 4,4'-bipyridine molecules. As discussed below, the result was the synthesis of the technically-new compound $(\text{bmim})_3[\text{PMo}_{12}\text{O}_{40}]$ (**3**).

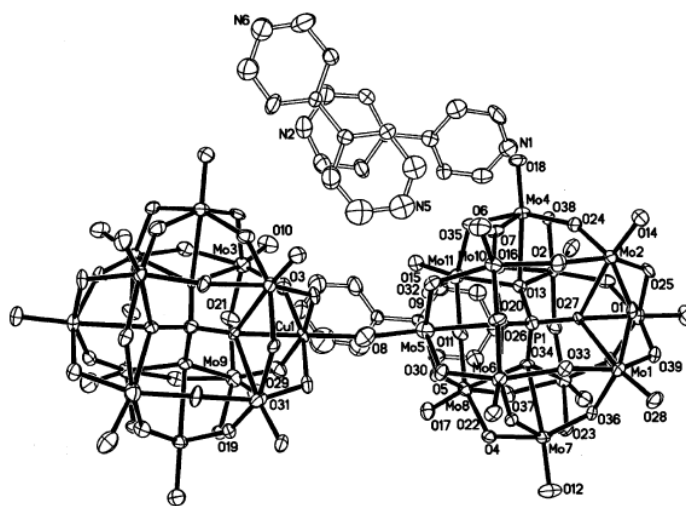


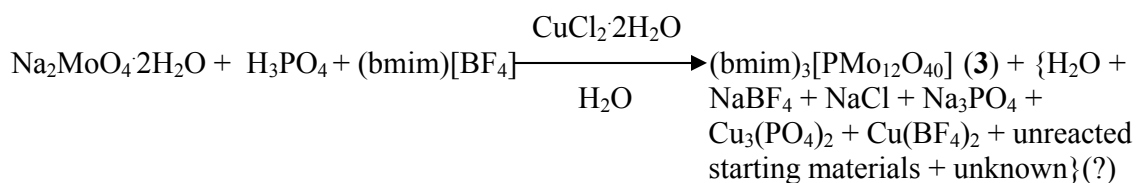
Fig. 3-1. ORTEP drawing of **1** showing the labeling of atoms with thermal ellipsoids at 50% probability. Hydrogen atoms are omitted for clarity.¹

(bmim)₃[PMo₁₂O₄₀] (3)

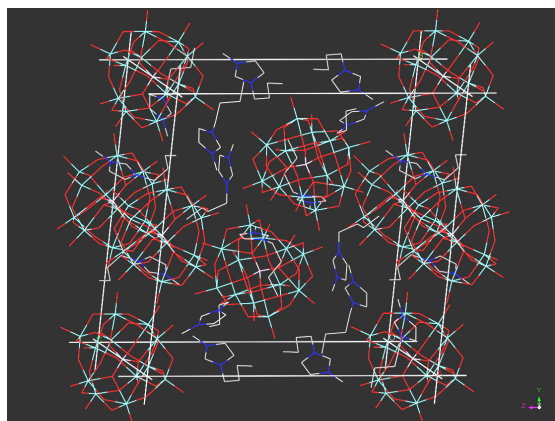
Synthesis and Crystal Structure

Yellow-green crystals of compound **3** with the formula (bmim)₃[PMo₁₂O₄₀] were obtained by me. This compound was initially obtained via the following ionothermal bomb reaction at 150 °C for seven days (Scheme 3-1).

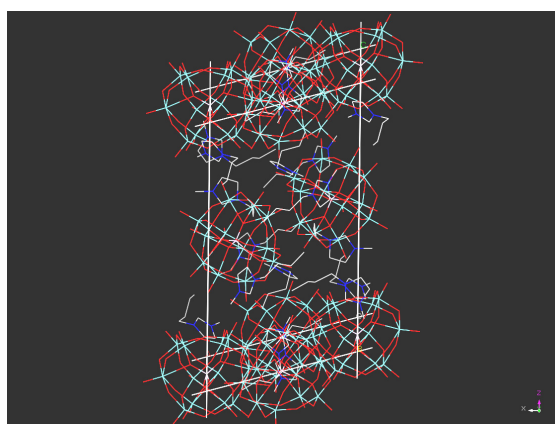
Scheme 3-1



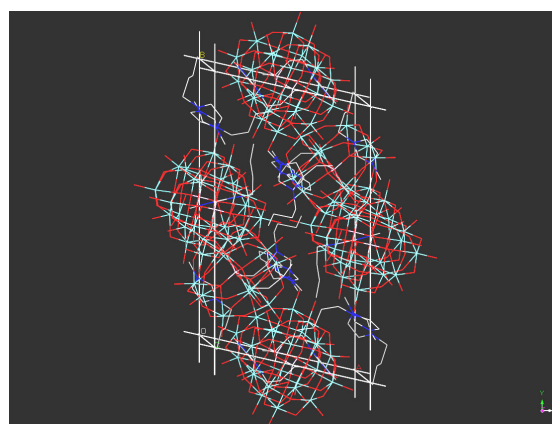
The single crystal x-ray diffraction analysis indicated that the compound crystallized in the triclinic space group P-1. The crystallographic asymmetric unit contains one Keggin anionic cluster (1 P, 12 Mo, 40 O) and three bmim molecules. The unit cell, which contains a total of four Keggin clusters (each carrying a 3- charge) and twelve bmim molecules (each carrying a +1 charge), is generated by applying inversion symmetry to the asymmetric unit. Three different views of the unit cell are shown in Figure 3-2 below.



(a)



(b)



(c)

Fig. 3-2. View of the unit cell of **3** projected approximately along the (a) x axis (b) y axis and (c) z axis. Disorder in the anionic Keggin clusters on the edges of the unit cell and in the cations is not shown for clarity. Color explanation: Light blue, Mo; Dark blue, N; Purple, P; Red, O; Grey, C.

Based on the descriptions given in Chapter 1, there are α -Keggin clusters in this compound. As for compound **2**, the Keggin clusters in compound **3** have approximate tetrahedral symmetry. The Mo–O distances range from 1.660(7)–2.449(4) Å. A closer inspection of the asymmetric unit reveals that the 36 Mo–O bonds involving 36 terminal oxygens range from 1.660(7)–1.696(7) Å, the 144 Mo–O bonds involving 72 doubly bridged oxygens range from 1.814(6)–2.032(4) Å, and the 36 Mo–O bonds involving 12 phosphate

oxygens range from 2.411(5)–2.449(4) Å. The 12 P–O bonds range from 1.505(3)–1.563(3) Å. These ranges for specific types of bonds generally agree with reported values for 3-charge phosphorus-containing α -Keggin molybdate compounds.²⁻⁵ Reference 3 combined all the bridging oxygens together into one range rather than create two separate ranges as we have done. Reference 5 discusses a Keggin structure which has cations originating from an ionic liquid, but the article only provides data pertaining to the P–O bonds. When we consider the unit cell, the Keggin clusters located on general sites inside the unit cell have no disordered atoms. All of the atoms of the Keggin clusters located on inversion sites on the unit cell edges have an occupancy of 0.5, except for the central phosphorus atom, which is not disordered. Compound **3** has 3 anion sites, whereas compounds **1** and **2** only have 1 anion site. Disorder is also present in five out of the six cations in the asymmetric unit. More specifically, three of the cations have disorder in all of their atoms, and two of the cations have disorder in the atoms of their butyl groups. Mo–O–Mo bond angles involving phosphate oxygen atoms range from 87.25(15)–90.88(19)°, while Mo–O–Mo bond angles involving bridging oxygen atoms range from 123.69(19)–127.2(4)° and from 150.7(4)–153.4(4)°. These bond angles agree with those reported in the literature.⁴ The O–P–O tetrahedral angles range from 108.8(2)–109.9(2)° for the ordered Keggin clusters, and from 104.0(2)–115.3(3)° for the disordered Keggin clusters. The ideal tetrahedral angle is 109.5°. Therefore, the PO₄ geometry of the ordered Keggin clusters is close to ideal, but some departure from ideality is observed in the geometry of the disordered Keggin clusters.

The P---P distances between two different Keggin clusters in the unit cell range from 11.288–31.814 Å. The 23 unique inter-ionic O---O distances in this structure range from 3.0059–4.01 Å. In addition, no hydrogen bonding is present in **3**. A summary of the crystal data for **3** is provided in Table 3-1 below.

Table 3-1 Crystal Data for (bmim)₃[PMo₁₂O₄₀]

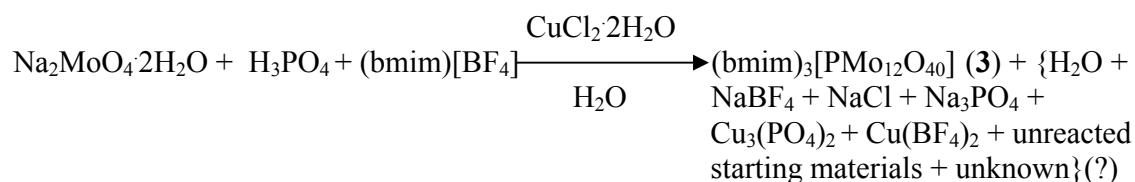
3	
Molecular formula	(bmim) ₃ [PMo ₁₂ O ₄₀]
FW	2239.91
Space group	<i>P</i> -1
a (Å)	12.8716(6)
b (Å)	21.1033(9)
c (Å)	21.6102(10)
α	96.282(1)
β	105.243(1)
γ	100.756(1)
V(Å ³)	5485.7(4)
Z	4
T, K	100(2)
λ, Å	0.71073
ρ _{calc} , gcm ⁻³	2.712
μ (mm ⁻¹)	2.780
R[F ² > 2σ(F ²)]	0.0573
wR(F ²)	0.1079

$$R = \frac{\sum ||F_o| - |F_c||}{\sum |F_o|}, \quad wR = \sqrt{\frac{\sum [w(F_o^2 - F_c^2)^2]}{\sum w(F_o^2)^2}}, \quad w = 1/[\sigma^2(F_o^2) + (0.0500P)^2 + 4.0000P],$$

$$P = (F_o^2 + 2F_c^2)/3$$

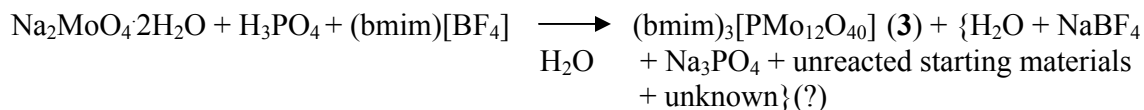
My best results were achieved via the following ionothermal bomb reaction at 150 °C for four days (Scheme 3-2).

Scheme 3-2



The question of whether compound **3** could be synthesized without copper chloride dihydrate was answered affirmatively via the following ionothermal bomb reaction at 150 °C for four days (Scheme 3-3).

Scheme 3-3



Interestingly, this reaction only had a yield of about 10 percent. In contrast, the reaction in Scheme 3-2, which provided the best results for this compound, had a yield of about 45 percent. These results prompted the question: “Does copper chloride play a role in this reaction?”

In an attempt to answer this question, reactions, which utilized different amounts of copper chloride dihydrate, were conducted, and a graph (see Figure 3-3 below) was created to help analyze the results.

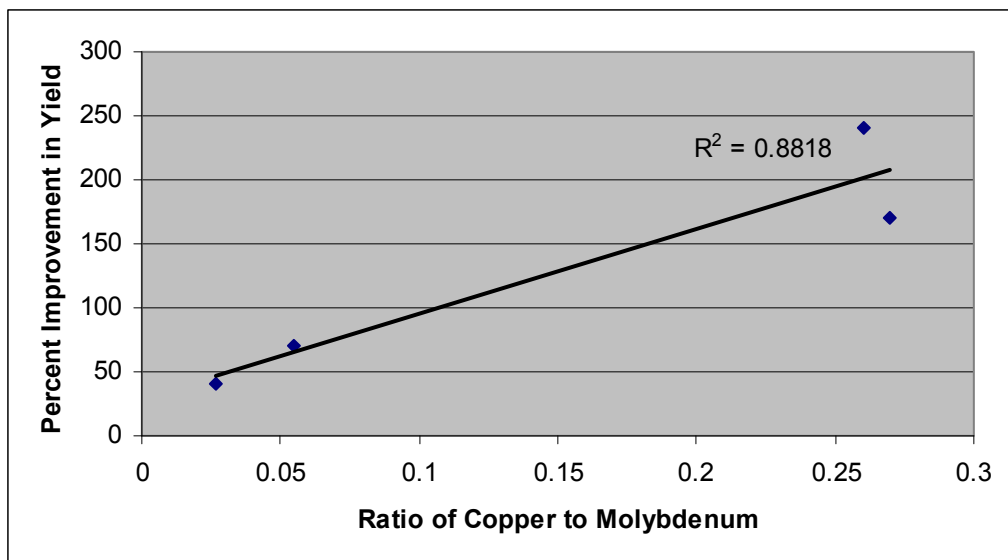


Fig. 3-3. Percent improvement in yield of compound **3** as a function of the copper to molybdenum ratio.

On the x-axis of this graph is the amount of moles of copper chloride dihydrate divided by the amount of moles of sodium molybdate, or the ratio of copper to molybdenum. On the y-axis is the percent improvement in yield of each reaction in relation to the yield of the reaction, in Scheme 3-3 referenced above, which did not have copper chloride. We see that there is a correlation between the amount of copper chloride dihydrate used and the improvement in yield. The correlation could be considered to be somewhat weak, because the R-squared value is only 0.88, but nevertheless a correlation does seem to exist. So generally speaking, copper chloride dihydrate does seem to have a positive impact on the formation of compound **3**. When more copper chloride dihydrate is used, we observe a higher yield.

There are sources of error that should be noted here. First, there is limited data. Only one reaction that did not have copper chloride was conducted, and only four other reactions are being compared with the no-copper reaction. The four reactions were chosen because they produced compound **3**, and because they were the most similar both to each other and also to

the no-copper reaction in terms of reaction conditions. Second, although the reactions are similar, they are not identical beyond the fact that different amounts of copper chloride were used. The reactions were not all done at the same time, or in the same oven, and the amounts of reagents were generally not identical. Third, we have to consider the purification of the products for each reaction. The reactions that have more copper chloride are generally more difficult to purify, because purification essentially involves segregating the copper-based impurities from the desired product on the filter paper during filtration. If more copper-based impurity is present, then segregation is less efficient, and some product needs to be left behind, reducing the effective yield. Fourth, even after segregating product from impurity, impurities still remain mixed in with the desired product. This causes yields to be overstated, because the purity of each product sample is not 100 percent. Fifth, we have experimental error. This category includes difficulties experienced during the weighing of the product obtained from one of the reactions (the one represented by the second data point from the left in the graph). Some of the product was spilled during weighing. Not all of it was recovered, and the amount that was recovered may have been contaminated somewhat. So the yield I arrived at for this reaction is only an estimation (although still a good estimation), and it has more error associated with it than the yields of the other reactions. Finally, since the yields were rounded, some rounding error will be present.

Error notwithstanding, the fact that the copper chloride seems to be improving the yield of these reactions seems inescapable. Which leaves us with the question: “How does copper chloride improve the yield?”

This question is difficult to answer definitively, but we can theorize and/or speculate using knowledge obtained from the article that inspired this work,¹ and from conversations with members of my research group. We know from the article that metal atoms can be removed from Keggin clusters, forming what are called “lacunary species.” This phenomenon makes

it possible to synthesize copper-substituted Keggin heteropolymolybdates, among other things. Perhaps when copper chloride is used in the compound **3** reactions, a copper-substituted Keggin compound is formed as an intermediate, and then over the course of the reaction the copper atom is replaced by a molybdenum atom, since molybdenum is much more prevalent in the reaction mixture. So in effect, the copper chloride is helping to form the desired product, which is admittedly quite complex, by providing a more favorable synthetic pathway, one which is not available if no copper chloride is used in the reaction. In order to prove this theory, a copper-containing intermediate would have to be isolated, which, depending on the lifetime of such an intermediate, may or may not be possible. The intermediate would have to be able to survive long enough to crystallize. It is also possible that some copper-containing crystals are obtained in the compound **3** reactions, and we were simply unlucky in choosing a crystal for structure determination that did not contain copper.

Characterization

A PXRD pattern, a TGA plot and a UV spectrum for **3** are shown in Fig. 3-4 below.

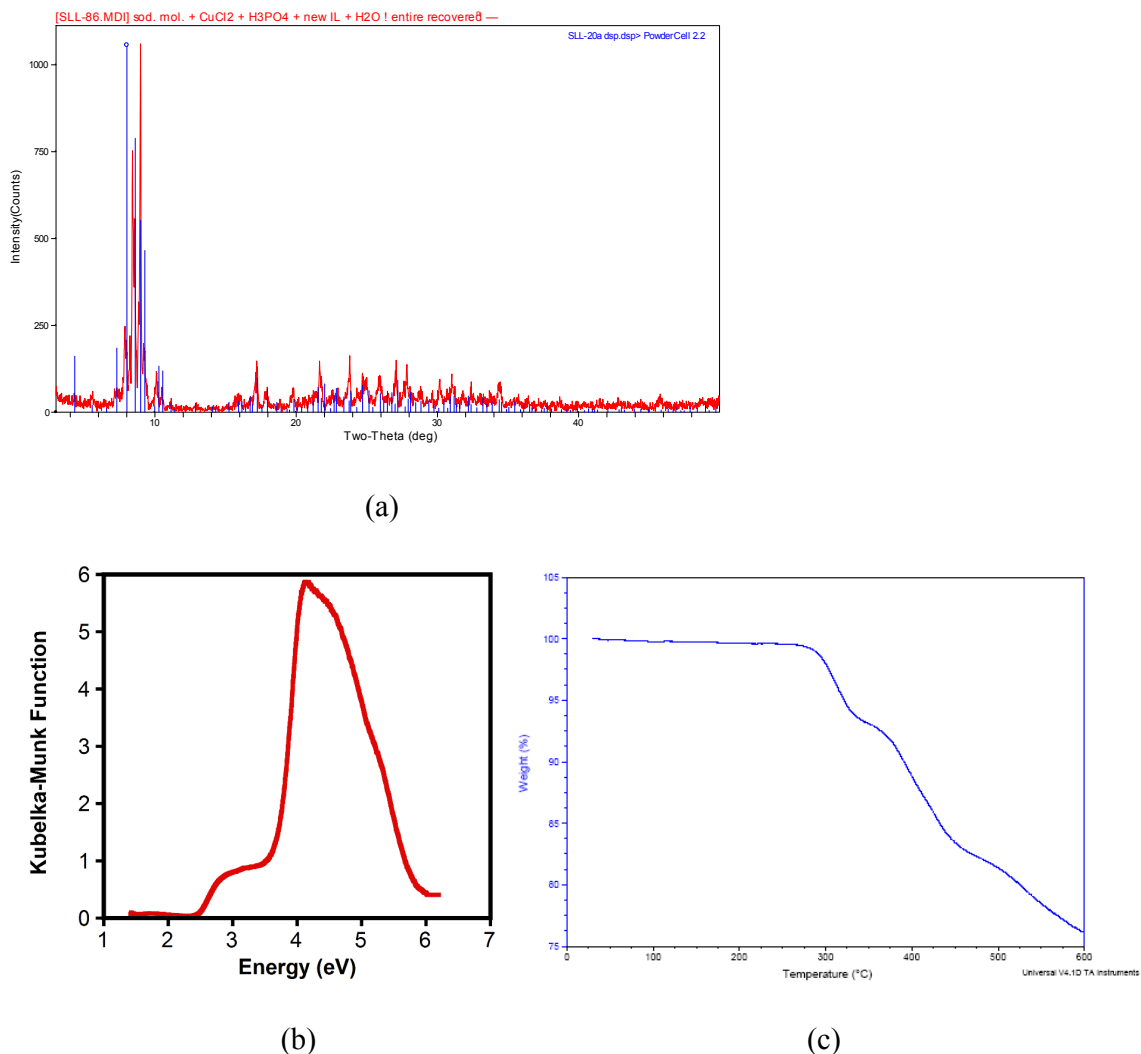


Fig. 3-4. (a) The PXRD pattern for **3**, where the red trace is the pattern generated from material obtained from a reaction which followed Scheme 3-2, and the blue trace is the simulated pattern generated from material from the Scheme 3-1 reaction (b) The UV spectrum for **3**, taken with pure material from both the Scheme 3-2 reaction and another reaction following the same scheme (c) The TGA plot for **3**, taken with some of the same material that the UV was taken with (approx. 7 mg of **3** heated at a rate of 5 °C/min)

As shown in Figure 3-4a, the simulated and experimental PXRD patterns match quite well, especially in the 2θ range of about 8–10. As shown in Figure 3-4b, the bandgap of

compound **3** is about 3.5 eV, which is indicative of a wide bandgap material. As shown in Figure 3-4c, compound **3** is thermally stable to approximately 280 °C.

It is interesting to compare compound **2** and compound **3**. This comparison is made in Table 3-2 shown below. Both compounds are Keggin-based, but compound **3** is much less symmetric and much more voluminous than compound **2**. The two compounds are indeed quite different.

Table 3-2 Crystal data comparison of **2** and **3**

	2	3
FW	2379.13	2239.91
Space group	P2 ₁ /n	P-1
a (Å)	13.159(3)	12.8716(6)
b (Å)	16.952(3)	21.1033(9)
c (Å)	14.383(3)	21.6102(10)
α	90.00	96.282(1)
β	91.45(3)	105.243(1)
γ	90.00	100.756(1)
V(Å ³)	3207.41(11)	5485.7(4)
Z	2	4
T, K	293(2)	100(2)
λ , Å	0.71073	0.71073
ρ_{calc} , gcm ⁻³	2.463	2.712
μ (mm ⁻¹)	2.386	2.780
R ($I > 2\sigma(I)$)	0.0278	0.0573
R _w	0.0659	0.1079

Catalysis

Synthesis and Recovery of catalyst

Compound **3** was used as a catalyst in oxidation reactions to convert styrene to benzaldehyde. The overall reaction is shown in Figure 3-5 below.

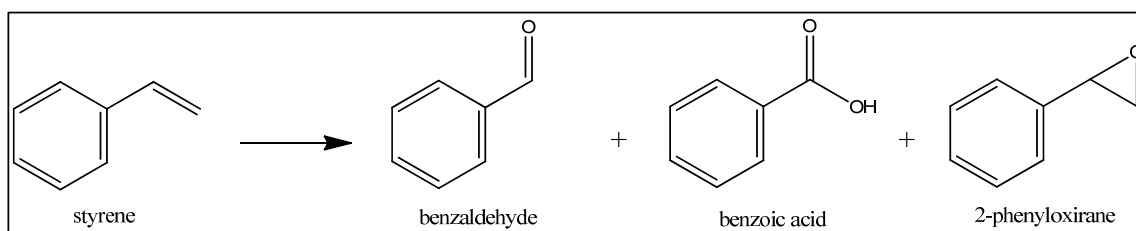


Fig. 3-5. Schematic representation of the reaction performed using compound **3** as an oxidation catalyst. Benzaldehyde is the major product, while benzoic acid and 2-phenyloxirane are minor products.

To achieve this conversion, 1 millimole of styrene, 2 millimoles of hydrogen peroxide, 0.0067 millimoles of compound **3**, and 10 mL of acetonitrile were added to a 50 mL round bottom flask. The contents of the flask were then stirred and heated in an oil bath at 70 °C for 12 hours. At the end of the reaction, the contents of the flask were characterized by gas chromatography. It should be noted that when this reaction was attempted using methanol as the solvent, no reaction was observed. This observation may be related to the fact that compound **3** is not soluble in methanol, but is soluble in acetonitrile. The reaction conditions described above afforded the best results.

An important aspect of this work was the recovery and reuse of the catalyst after the reactions. To do this, the acetonitrile was removed from the round bottom flask with a rotary evaporator. A red-colored gel remained in the flask after evaporation. Methanol was slowly added to this gel, which caused the catalyst to precipitate out. The solution was then centrifuged. Afterwards, the methanol in the centrifuge tube was decanted, and 5 mL of

additional methanol were added to it. This new solution was then centrifuged again to recover more catalyst. This procedure was followed after each reaction, and the recovered catalyst material was used in the subsequent reaction. These procedures made it possible to conduct a total of five separate oxidation reactions using the same catalyst material. 0.0067 millimoles of catalyst were used for the first reaction, and then the amount of catalyst that was recovered after each reaction was used to conduct the subsequent reaction (after the first reaction, the amount of catalyst used was not determined).

Discussion of Results

The results that were obtained are summarized in Table 3-3 below. As shown in the table, the reaction is highly selective for benzaldehyde, and a decrease in selectivity of only 2.5% is observed after five reactions with the same catalyst material. The styrene conversion is also relatively high, although it does decrease rather significantly from the first reaction to the fifth. This is at least partially due to the fact that catalyst material was lost each time a GC sample was obtained. Regarding the minor products, we observe that initially 2-phenyloxirane is the predominant minor product, but after five reactions, benzoic acid is the predominant minor product. It should also be noted that the compound **3** material used in these reactions was synthesized without copper chloride dihydrate. Therefore, the results have not been skewed by any copper-based impurity, which could theoretically provide additional catalytic activity on its own.

Table 3-3 Results of styrene oxidation reactions

Reaction	Number of recycles	Styrene conversion (%)	Selectivity (%)		
			Benzaldehyde	Benzoic acid	2- phenyloxirane
1	0	83	96.5	1	2.5
2	1	80.5	95	2	3
3	2	80.5	96	2	2
4	3	76.3	94.4	4.1	2.5
5	4	69.4	94	4.2	1.8

As the PXRD patterns in Figure 3-6 below show, the catalyst is essentially unchanged after being used in five oxidation reactions. This indicates that the catalyst is highly robust and therefore quite useful for this particular application. Further verification of the robust nature of this compound is given in Figure 3-7 below, which shows the TGA spectrum of material not used in catalysis reactions as well as the TGA spectrum of the material which was used in five catalysis reactions. The two spectra were taken with different batches of compound **3**, but a comparison is still appropriate. For the most part, the two spectra have the same general features, although the one in Figure 3-7b does have an extra weight loss between approximately 50 °C and approximately 280 °C. This may be due to the presence of impurities, which were introduced during the catalytic reactions, and which were not removed prior to obtaining the TGA spectrum.

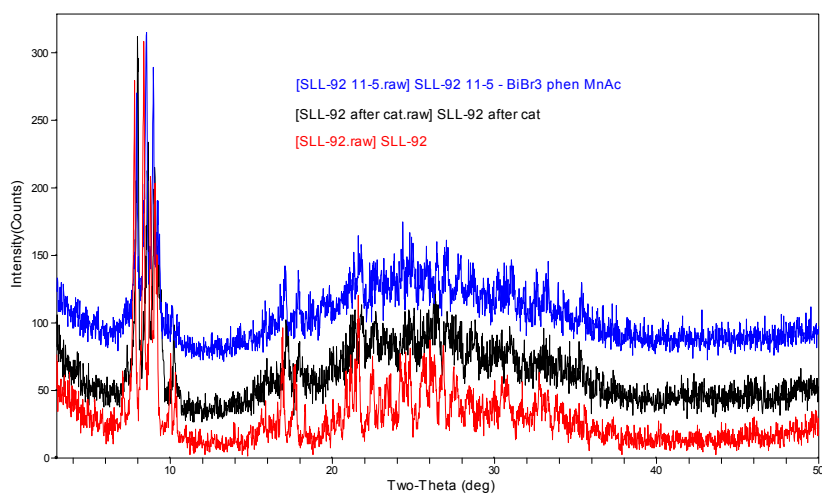


Fig. 3-6. PXRD pattern of compound **3** before oxidation reactions (red trace), after one oxidation reaction (black trace), and after five oxidation reactions (blue trace).

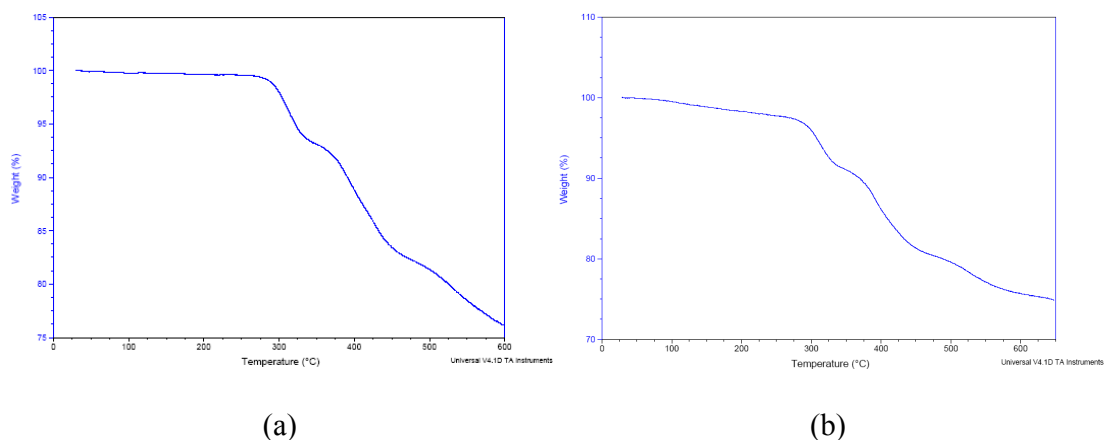


Fig. 3-7. (a) The TGA plot for unused compound **3** material (the same spectrum shown in Fig. 3-4) (b) The TGA plot for compound **3** material used in five catalysis reactions (approx. 5 mg of **3** heated at a rate of 5 °C/min). Note the difference in scale between the two plots.

How do these results compare with values reported in the literature? The liquid-phase oxidation of styrene to benzaldehyde has been catalyzed in a variety of ways.⁶⁻¹⁴ Catalysts that have been used include mesoporous molecular sieves, polyoxometalates, and Wilkinson's complex. Among the cited references (which do not constitute an exhaustive

list), the best performance in terms of the combination of conversion and selectivity seems to have been afforded by the authors of reference 7. The authors used the polyoxometalate $[\text{Co}(\text{H}_2\text{O})_6]_2\{[\text{Co}(\text{H}_2\text{O})_4]_2[\text{Co}(\text{H}_2\text{O})_5]_2\text{WZn}[\text{Co}(\text{H}_2\text{O})]_2(\text{ZnW}_9\text{O}_{34})_2\} \cdot 10\text{H}_2\text{O}$, the oxidant H_2O_2 , and the solvent acetone at 50 °C for 12 hours. These conditions yielded a styrene conversion of 96% and a benzaldehyde selectivity of 99%. Both of these values exceed the best values obtained using compound **3**. Regarding reusability, the best performance seems to have been afforded by the authors of reference 8 (reusability information was only obtained for three of the cited references). The authors used a water-soluble Pd complex as the catalyst, O_2 gas as the oxidant, and water as the solvent at 80 °C for 12 hours. After eight reactions, the styrene conversion was 96.4% and the benzaldehyde selectivity was 78.4%. Since the authors of reference 8 did eight reactions instead of only five as we did, a direct comparison with our results is problematic. Nevertheless, we do notice that their final conversion percentage was much better than ours, and simultaneously that their final selectivity was significantly lower than ours.

Summary

A technically-new polyoxomolybdate compound was synthesized during efforts to produce a copper-substituted Keggin-based structure. This work was motivated by a journal article found in the literature. Compound **3** was synthesized with (bmim)[BF₄], sodium molybdate, phosphoric acid, and water. Incorporation of copper into the Keggin clusters was not observed. However, copper chloride dihydrate did have an impact on the outcome of the reactions. It was observed that there was a fairly strong correlation between the copper-to-molybdenum ratio and the yield of the reaction. It is unclear what role the copper chloride dihydrate plays in the reaction, since **3** could be synthesized with or without it, but a copper-substituted intermediate may be involved.

Compound **3** contains three imidazolium cations for every Keggin cluster to balance the negative charge of the clusters. No hydrogen bonding exists in the structure. The Keggin clusters inside the unit cell have no disorder, but disorder is present in the Keggin clusters on the unit cell edges. Disorder is also present in most of the imidazolium cations.

Compound **3** was used as a catalyst in reactions to oxidize styrene to benzaldehyde, and the results were quite good. It was also demonstrated that compound **3** could be reused multiple times without altering its structure. The catalysis results indicate that compound **3** is a suitable catalyst for the synthesis of benzaldehyde.

References

- (1) Lu, Y.; Xu, Y.; Wang, E.; Li, Y.; Wang, L.; Hu, C.; Xu, L. *J. Solid State Chem.* 2004, *177*, 2210-2215.
- (2) Gong, Y.; Hu, C.; Li, H.; Tang, W.; Huang, K.; Hou, W. *J. Mol. Struct.* 2006, *784*, 228-238.
- (3) Li, J.; Qi, Y.; Li, J.; Wang, H.; Wu, X.; Duan, L.; Wang, E. *J. Coord. Chem.* 2004, *57*, 1309-1319.
- (4) Zhai, Q.; Wu, X.; Chen, S.; Zhao, Z.; Lu, C. *Inorg. Chem.* 2007, *46*, 5046-5058.
- (5) Rao, G. R.; Rajkumar, T; Varghese, B. *Solid State Sci.* 2009, *11*, 36-42.
- (6) Wei, T.; Li, J.; Shen, J.; Duan, D.; Chen, N. *Huagong Keji* 2009, *17*, 21-25.
- (7) Tang, J.; Yang, X.; Zhang, X.; Wang, M.; Wu, C. *Dalton Trans.* 2010, *39*, 3396-3399.
- (8) Feng, B.; Hou, Z.; Wang, X.; Hu, Y.; Li, H.; Qiao, Y. *Green Chem.* 2009, *11*, 1446-1452.
- (9) Hu, J.; Li, K.; Li, W.; Ma, F.; Guo, Y. *Appl. Catal., A* 2009, *364*, 211-220.
- (10) Liu, J.; Wang, F.; Gu, Z.; Xu, X. *Chem. Eng. J.* 2009, *151*, 319-323.
- (11) Li, J.; Yin, D.; Xu, Q.; Guo, J.; Zhou, H.; Chen, M. *Huagong Jinzhan* 2008, *27*, 1096-1099, 1136.
- (12) Bai, L.; Lei, F.; Mo, L.; Luo, Y.; Huang, Y. *Linchan Huaxue Yu Gongye* 2007, *27*, 99-104.
- (13) Gao, D.; Gao, Q. *Catal. Commun.* 2007, *8*, 681-685.
- (14) Yogish, K.; Sastri, N. V. S. *Ind. Eng. Chem. Res.* 1988, *27*, 909-915.

EXPERIMENTAL

Materials and Instruments

The following reagents used specifically in my work were commercially purchased and used as received.

(bmim)[BF ₄]	1-butyl-3-methyl-imidazolium tetrafluoroborate BASF, Sigma-Aldrich >98% (Compound 2 and last 2 reactions for 3)
(NH ₄) ₆ Mo ₇ O ₂₄ ·4H ₂ O	Ammonium molybdate tetrahydrate (para) Alfa Aesar ACS grade
NH ₄ H ₂ PO ₄	Ammonium phosphate monobasic J.T. Baker 99.66%
CuCl ₂ ·2H ₂ O	Copper (II) chloride dihydrate Alfa Aesar 99.999% (1st 3 reaction)
CuCl ₂ ·2H ₂ O	Copper (II) chloride dihydrate Aldrich 99+% (2 nd 3 reaction)
MeOH	Methanol, dried BDH analytical solution (last 2 reactions for 3)
H ₃ PO ₄	Phosphoric acid Acros Organics 85 wt% in water
Na ₂ MoO ₄ ·2H ₂ O	Sodium molybdate dihydrate Fisher Scientific 102%
Other reagents mentioned in this section.	
2-pca	2-pyridinecarboxylic acid
La(OH) ₃	Lanthanum hydroxide

Powder X-ray diffraction (PXRD) spectra were obtained using a Rigaku D/Max-2200T automated diffraction system (Ultima⁺), or a Rigaku Ultima IV automated diffraction system. The structures were analyzed with JADE and PowderCell2.2.

Single crystal X-ray diffraction experiments were conducted on a Bruker-AXS SMART APEX CCD diffractometer with graphite-monochromated Mo K α radiation, or a Nonius CAD4 diffractometer with graphite-monochromated Mo K α radiation. The structures were solved using the SHELXS-97 crystallographic software package, and the structures were refined using the SHELXL-97 crystallographic software package.

Thermogravimetric (TG) analyses were conducted on a Q50 thermogravimetric analyzer.

Synthesis of (bmim)₃NH₄[Mo₈O₂₆] (1)

Samantha Levine conducted the ionothermal bomb reaction of 122.9 mg of (NH₄)₆Mo₇O₂₄·4H₂O (0.1 mmol), 18.3 mg of La(OH)₃ (0.1 mmol), 13.2 mg of 2-pca (0.1 mmol), and 14 drops of (bmim)[BF₄] (approximately 0.2 mL) at 140 °C in an acid digestion bomb for approximately six days. The bomb was allowed to cool in the oven. Large colorless crystals of (1) were obtained, along with white powder. The yield was not specified.

My best results were obtained by conducting the ionothermal glass vial reaction of 121.8 mg of (NH₄)₆Mo₇O₂₄·4H₂O (0.1 mmol) and 26 total drops of (bmim)[BF₄] (approximately 0.4 total mL) at 120 °C in a 20 mL glass vial for approximately seven days. The vial was allowed to cool to room temperature naturally. Colorless, shiny block crystals of (1) were isolated via filtration with MeOH, and further purification with distilled water and MeOH. The yield was 69% before the product was purified with distilled water.

Synthesis of (bmim)₄[PMo^VMo₁₁O₄₀] (2)

Samantha Levine conducted the ionothermal bomb reaction of 121.5 mg of (NH₄)₆Mo₇O₂₄·4H₂O (0.1 mmol), 19.5 mg of La(OH)₃ (0.1 mmol), 11.1 mg of NH₄H₂PO₄ (0.1 mmol), and 17 drops of (bmim)[BF₄] (approximately 0.2 mL) at 135 °C in an acid digestion bomb for approximately six days. The bomb was allowed to cool in the oven. Block blue crystals of (2) were obtained, along with colorless crystals and blue powder. The yield was not specified.

Moothetty Padmanabhan achieved excellent results by conducting the ionothermal glass vial reaction of 133.0 mg of $(\text{NH}_4)_6\text{Mo}_7\text{O}_{24}\cdot 4\text{H}_2\text{O}$ (0.1 mmol), 58.0 mg of $\text{NH}_4\text{H}_2\text{PO}_4$ (0.5 mmol), and 25 drops of $(\text{bmim})[\text{BF}_4]$ (approximately 0.4 mL) at 120 °C in a glass vial for approximately four days. Highly-pure blue powder of **(2)** was obtained in 78% yield.

My best results were obtained by conducting the ionothermal bomb reaction of 121.5 mg of $(\text{NH}_4)_6\text{Mo}_7\text{O}_{24}\cdot 4\text{H}_2\text{O}$ (0.1 mmol), 12.6 mg of $\text{NH}_4\text{H}_2\text{PO}_4$ (0.1 mmol), and 17 drops of $(\text{bmim})[\text{BF}_4]$ (approximately 0.2 mL) at 140 °C in a 23 mL acid digestion bomb for approximately seven days. These conditions were partially inspired by those used by Samantha Levine (see above). The bomb was placed on top of an air conditioning vent for rapid cooling. The products were filtered and washed with distilled water and methanol. Dark crystals of **(2)** were obtained, along with a variety of other products. Since multiple products were obtained, an accurate yield for **(2)** cannot be determined.

Synthesis of $(\text{bmim})_3[\text{PMo}_{12}\text{O}_{40}]$ (3**)**

This compound was first obtained by conducting the ionothermal bomb reaction of 69.3 mg of $\text{Na}_2\text{MoO}_4\cdot 2\text{H}_2\text{O}$ (0.3 mmol), 13.6 mg of $\text{CuCl}_2\cdot 2\text{H}_2\text{O}$ (0.1 mmol), 75.8 mg of H_3PO_4 (0.7 mmol), five drops of distilled water (approximately 0.5 mL), and 30 drops of $(\text{bmim})[\text{BF}_4]$ (approximately 0.4 mL) at 150 °C in a 23 mL acid digestion bomb for seven days. The bomb cooled in a 120 °C oven, followed by a 100 °C oven, and finally on the benchtop at RT. The total cooling time was approx. 6.5 hours. The products were filtered and washed with methanol. After air-drying, the desired product crystals were further purified with distilled water and methanol. Yellow-green crystals of **(3)** were obtained in undetermined yield, along with a small amount of blue and black impurities.

My best results were obtained by conducting the ionothermal bomb reaction of 69.6 mg of $\text{Na}_2\text{MoO}_4 \cdot 2\text{H}_2\text{O}$ (0.3 mmol), 13.5 mg of $\text{CuCl}_2 \cdot 2\text{H}_2\text{O}$ (0.1 mmol), 83.7 mg of H_3PO_4 (0.7 mmol), five drops of distilled water (approximately 0.5 mL), and 30 drops of (bmim)[BF_4] (approximately 0.4 mL) at 150 °C in a 23 mL acid digestion bomb for four days. The bomb cooled in the oven at the rate of 0.1 °C/min to around 45 °C, and was then placed on top of an air conditioning vent to finish cooling. The products were filtered and washed with distilled water and methanol. After air-drying, the desired product crystals were further purified with distilled water and methanol. Yellow-green crystals of (**3**) were obtained in 45% yield. Some blue impurity was present.

This compound was also synthesized without copper chloride dihydrate. This was achieved by conducting the ionothermal bomb reaction of 351 mg of $\text{Na}_2\text{MoO}_4 \cdot 2\text{H}_2\text{O}$ (1.5 mmol), 404 mg of H_3PO_4 (3.5 mmol), 25 drops of distilled water (approximately 2.5 mL), and 150 drops of (bmim)[BF_4] (approximately 2.1 mL) at 150 °C in a 23 mL acid digestion bomb for four days. The bomb cooled in a different oven which started at approx. 150 °C, but was turned off at the beginning of cooling. The products were filtered and washed with distilled water and methanol. After air-drying, further purification with distilled water and methanol was conducted. Yellow-green crystals of (**3**) were obtained in 10% yield. Some white or beige impurity was present.

Crystal Structure Analysis of 1

The data was collected on a Bruker-AXS SMART APEX CCD diffractometer with graphite-monochromated Mo K α radiation at 100(2) K. The SHELXS-97 crystallographic software package was utilized to solve the structure, and the SHELXL-97 crystallographic software package was utilized to refine the structure.

Crystal Structure Analysis of 2

The data was collected on a Nonius CAD4 diffractometer with graphite-monochromated Mo K α radiation at 293(2) K. The SHELXS-97 crystallographic software package was utilized to solve the structure, and the SHELXL-97 crystallographic software package was utilized to refine the structure.

Crystal Structure Analysis of 3

The data was collected on a Bruker-AXS SMART APEX CCD diffractometer with graphite-monochromated Mo K α radiation at 100(2) K. The SHELXS-97 crystallographic software package was utilized to solve the structure, and the SHELXL-97 crystallographic software package was utilized to refine the structure.

PXRD Analysis

PXRD spectra were obtained using a Rigaku D/Max-2200T automated diffraction system (Ultima⁺) with graphite-monochromated Cu K α radiation, or a Rigaku Ultima IV automated diffraction system with graphite-monochromated Cu K α radiation. The 2θ range utilized was 3-50°. Spectra were obtained at room temperature at the operating power of 40 kV/40 mA or 40kV/44 mA.

Thermal Analysis

Thermogravimetric (TG) analyses were conducted on a Q50 thermogravimetric analyzer under nitrogen. The samples (3-7 mg) were loaded into platinum pans and heated at a rate of 5 °C/min from room temperature to at least 600 °C.